

# Periodic vacuum and particles in two dimensions

Marianne Dufour Fournier\*

*Institut de Recherches Subatomiques*

*F67037 Strasbourg Cedex 2 BP 28, France*

Janos Polonyi†

*Laboratory of Theoretical Physics, Louis Pasteur University*

*3 rue de l'Université 67087 Strasbourg, Cedex, France*

*and*

*Department of Atomic Physics, L. Eötvös University*

*Puskin u. 5-7 1088 Budapest, Hungary*

(September 2, 2018)

## Abstract

Different dynamical symmetry breaking patterns are explored for the two dimensional  $\phi^4$  model with higher order derivative terms. The one-loop saddle point expansion predicts a rather involved phase structure and a new Gaussian critical line. This vacuum structure is corroborated by the Monte Carlo method, as well. Analogies with the structure of solids, the density wave phases and the effects of the quenched impurities are mentioned.

## I. INTRODUCTION

The condensates occurring in Quantum Field Theory are usually homogeneous and are composed of particles with vanishing momentum. In this manner the momentum of the excitations is conserved even when a particle is borrowed from or lended to the vacuum. But the momentum conservation observed experimentally at finite energies is actually not incompatible with certain inhomogeneous vacua so long as the momentum of the condensed particles is beyond the observational range. The elementary excitations in solids are described by the Bloch waves which can be rearranged into different sub-Brillouin zones in such a manner that the Bloch momentum, the momentum counted from the center of the sub-Brillouin zone, is conserved. More formally, the presence of a crystalline ground state restricts the translations as symmetries such that the primitive unit cells are mapped into each other. The conserved quantum number due to such a restricted symmetry group is

---

\*Marianne.Dufour@IReS.in2p3.fr

†polonyi@fresnel.u-strasbg.fr

the Bloch momentum. The umklapp processes which take place at the length scale of the primitive unit cell change the sub-Brillouin zone and can be interpreted as a change of the type of the excitations. Returning now to Quantum Field Theory, one might send the size of the primitive unit cell to zero. If this is possible then the space-time structure of the momentum non-conserving umklapp process is not resolved by finite measurements and their interpretation as a flavor changing process becomes compatible with the experiments.

In order to gain more insight into the role the inhomogeneity of the vacuum plays in forming the dynamics of the excitations we consider a generic model for a scalar field in two dimensions and present its phase structure, the excitation spectrum and the particle content when the vacuum possesses a modulation and becomes inhomogeneous. We use the saddle point approximation in the one-loop order in the analytical computation and the Monte Carlo for the numerical simulation to have a more complete picture.

The organization of the paper is the following. Section II contains our motivation in choosing the model investigated. The tree level vacuum is identified in Section III. The action is rewritten in terms of the Bloch waves corresponding to the different periodic vacua in Section IV. We diagonalize the quadratic part of the action and determine the elementary excitations for the simplest inhomogeneous vacuum in Section V. Section VI contains the demonstration of the one-loop renormalizability of our model. The analytical results are compared with a Monte Carlo computation in Section VII. Finally Section VIII is for the conclusions.

## II. THE MODEL

Our model is an extension of the Landau-Ginzburg model for a scalar order parameter by adding higher order derivatives to the action,

$$S[\phi(x)] = \int d^d x \left\{ \frac{1}{2} \partial_\mu \phi(x) \mathcal{K} \left( \frac{(2\pi)^2}{\Lambda^2} \square \right) \partial_\mu \phi(x) + V(\phi(x)) \right\}, \quad (1)$$

where the kinetic energy contains the functions

$$\mathcal{K}(z) = 1 + c_2 z + c_4 z^2, \quad V(\phi) = \frac{m^2}{2} \phi^2 + \frac{\lambda}{4} \phi^4, \quad (2)$$

and  $\Lambda$  is the ultraviolet cutoff.

As far as the dimensionless parameters  $c_2$  and  $c_4$  are concerned, we have two different motivations for their introduction. One is based on the fact that we are always confronted in Nature with effective theories where the high energy particle exchanges generate a number of operators in the action which are perturbatively non-renormalizable. As an example, consider a renormalizable model for a heavy and light particle, described by the fields  $\Phi$  and  $\phi$ , respectively and the bare action  $S_0[\phi, \Phi]$ . The effective action for the asymptotic states below the threshold of the heavy particle is given by  $S_{eff}[\phi] = S_0[\phi, \Phi = 0] + \Delta S[\phi]$ , where  $\Delta S[\phi]$  contains all effective vertices generated by the heavy particle exchange processes. In this manner we can never be sure that the action corresponding to the interactions in a given energy range is actually limited by the renormalizability even though the "Theory of Everything" is supposed to be finite or renormalizable. The higher order derivative

terms of our model may arise from  $\Delta S[\phi]$ . The decoupling theorem, [1], helps us out from the problem of a too general action with non-renormalizable terms by asserting that the non-renormalizable coupling constants are small, being suppressed by the power of the light and the heavy particle mass ratio. The question, left open by the conclusion of the decoupling theorem, and which motivates the present work is whether the smallness of the non-renormalizable coupling constants is really sufficient to render them unimportant in the effective theory. We shall find that certain higher order derivative terms may become relevant when their coupling constants exceed a threshold value. In other words, we might be forced to consider non-renormalizable terms in our effective theories if the heavy particle is not exceedingly far from the observational energy. The other motivation to study the model (1) with non-renormalizable terms is the suspicion that the perturbatively non-renormalizable terms might turn out to be relevant by a non-perturbative mechanism and actually allow the removal of the cutoff. If this is happened to be the case then our model with non-vanishing  $c_2$  and  $c_4$  is as justified as the usual one whose action is quadratic in the gradient.

What kind of heavy particle exchange is behind the higher order derivative terms of our action? As mentioned above, our interest is in theories with inhomogeneous vacuum. Such a ground state which is modulated with a period length  $\lambda_{vac}$  is the result of a force which is attractive for  $x > \lambda_{vac}$  and repulsive when  $x < \lambda_{vac}$ . When the particle whose exchange generates this force is eliminated, its effects are kept in the choice of the vertices in  $\Delta S[\phi]$ . The momentum independent ultra-local (i.e. non-derivative) terms which contribute to the local potential in the action can not generate such a strong distance dependence in the interaction. But it is easy to see that the higher order terms in the derivative are just for this role, to lower the action for modes whose characteristic momentum scale is  $p \approx 1/\lambda_{vac}$ . In fact, consider the eigenvalues of the second functional derivative of the action evaluated in the trivial vacuum  $\langle \phi(x) \rangle = 0$ ,

$$\epsilon(p) = V''(0) + p^2 \mathcal{K} \left( -\frac{(2\pi)^2}{\Lambda^2} p^2 \right). \quad (3)$$

The  $O(p^4)$  term produces a non-trivial local minimum at  $p = p_{min} \approx \lambda_{vac}^{-1}$  for  $c_2, c_4 > 0$ . Thus  $c_2$  and  $c_4$  correspond to a van der Waals force. We shall go further in this work and ask what happens when  $c_2$  reaches so large values that the minimum of the dispersion relation  $\epsilon(p)$  turns out to be negative. The corresponding vacuum will be the condensate of particles with momentum around  $p_{min}$  and will display the period length  $\lambda_{vac} \approx p_{min}^{-1}$ .

The hand-waving argument to retain the higher order derivative terms of (1) from the multitude of other contributions in  $\Delta S[\phi]$  is the following. Let us start with  $c_4 = 0$ , when the vacuum is homogeneous for  $c_2 < 0$ . On the contrary, for  $c_2 > 0$  an instability opens by increasing the momentum of the condensed particles and the ultraviolet cutoff stabilizes the vacuum [2] where particles with momentum at the cutoff are found. Models with such an instability were studied in refs. [3], [4] and [5] in three and four dimensions. If the inhomogeneous vacuum is supposed to be formed at momentum scales below the cutoff then we need another stabilization mechanism. For this end we retain the  $O(\partial^6)$  term with  $c_4 > 0$ . We believe that the higher order terms in the gradient will modify the shape of the saddle point only leaving the qualitative features of the inhomogeneous vacuum unchanged. In other words, the kinetic energy is generic. The present work can be considered as the

continuation of Ref. [5] where a new gaussian ultraviolet fixed point was found in the one-loop approximation for  $c_4 = 0$ . We simplify in this work the issue of the renormalizability by choosing lower dimension,  $d = 2$ , but the multitude of different phases is explored by allowing  $c_4 \neq 0$ .

The allusion made above at the Landau-Ginzburg model is based on the similarity of the functions  $V(u)$  and  $\mathcal{K}(u)$ . The nontrivial absolute minima provide the mechanism of the spontaneous ( $p = 0$ ) or dynamical ( $p \neq 0$ ) symmetry breaking generated by the potential in the internal space or the kinetic energy in the external (and internal) space, respectively. Our interest in this work is to explore the different dynamical symmetry breaking patterns provided by the generic action (1) and to suggest a mean-field treatment for the phase transitions with modulated ground state [6].

The questions addressed here and their tentative answers have certain relevance both in Solid State and High Energy Physics. The nontrivial, periodic vacuum generated by the higher order derivative terms may offer a new point of view in understanding the origin of the crystalline structure in solids. In fact, consider the coupled system of electrons, ions and photons. It is already an effective theory because the lower lying electrons of the ions are represented by the insertion of different charge distributions and form factors for the ions. We introduce chemical potentials for the electrons and the ions in order to realize electrically neutral matter with finite density. Finally we eliminate the heaviest degrees of freedom, the ions. This is opposite to the usual Born-Oppenheimer approximation but it generates a local effective interaction. This effective theory for electrons and photons contains higher order derivative terms for the photon field which yields the periodic, crystalline ground state. Another appearances of this mechanism where strong van der Waals forces are acting are the antiferromagnets and the charge or density wave phases. In the latter the effective theory is obtained by eliminating the valence electrons and has periodic tree level ground state [7]. The massless case with  $\epsilon(p_{min}) > 0$  may as well represent a superfluid system with  $p_{min}$  as the roton momentum [8]. In this context our quantitative argument showing the relation between the van der Waals forces and the higher order derivatives in the action represents a simple, effective theory motivated alternative of Feynman's argument about the rotons [9]. The instability leading to the formation of an inhomogeneous ground state when  $\epsilon(p_{min}) < 0$  is a quantum phase transition where a non-classical soft mode [11] shows up at  $p \approx p_{min}$ .

The periodic vacuum of our model supports frustrations for certain choice of the coupling constants. To see this we write the lattice regularized version of (1) in the form

$$\begin{aligned}
S[\phi(x)] &= \sum_x \left\{ -\frac{1}{2} \phi(x) \square \mathcal{K}(\square) \phi(x) + V(\phi(x)) \right\} \\
&= \sum_x \left\{ \phi(x) \left[ A\phi(x) + \sum_{\mu} \left( B(\phi(x + e_{\mu}) + \phi(x - e_{\mu})) \right. \right. \right. \\
&\quad \left. \left. \left. + C(\phi(x + 2e_{\mu}) + \phi(x - 2e_{\mu})) + D(\phi(x + 3e_{\mu}) + \phi(x - 3e_{\mu})) \right) \right. \right. \\
&\quad \left. \left. + \sum_{\mu < \nu} \left( E(\phi(x + e_{\mu} + e_{\nu}) + 2\phi(x + e_{\mu} - e_{\nu}) + \phi(x - e_{\mu} - e_{\nu})) \right. \right. \right. \\
&\quad \left. \left. \left. + F(\phi(x + 2e_{\mu} + e_{\nu}) + \phi(x + 2e_{\mu} - e_{\nu}) + \phi(x - 2e_{\mu} + e_{\nu}) \right. \right. \right. \\
&\quad \left. \left. \left. + \phi(x - 2e_{\mu} - e_{\nu})) \right) \right] \right\}
\end{aligned} \tag{4}$$

$$\begin{aligned}
& + G \sum_{\mu \neq \nu \neq \rho} \left( \phi(x + e_\mu + e_\nu + e_\rho) + 3\phi(x + e_\mu + e_\nu - e_\rho) \right. \\
& \left. + 3\phi(x + e_\mu - e_\nu - e_\rho) + \phi(x - e_\mu - e_\nu - e_\rho) \right) \Big] + \frac{\lambda}{4} \phi^4(x) \Big\},
\end{aligned}$$

where  $A = m^2/2 + d - (2d^2 + d)c_2 + (4d^3 + 6d^2)c_4$ ,  $B = -1/2 + 2dc_2 - (6d^2 + 3d - 3/2)c_4$ ,  $C = E/2 = -c_2/2 + 3dc_4$  and  $D = F/3 = G = -c_4/2$ . The possibility of having either sign for these coefficients indicates the competition between the nearest- and beyond nearest-neighbor interactions and the possible presence of frustrations as lattice defects of the periodic vacuum. When the amplitude of the periodic vacuum is large the motion of the frustration is rather slow and the model offers a semiclassical description of the quenched disorder.

The usual strategy in High Energy Physics is to introduce a field variable for each particles. But models with inhomogeneous vacua may display more involved particle-field assignments by exploiting the non-trivial dynamics at the ultraviolet cutoff scale. In fact, there are several dispersion relations and particle like-elementary excitations in Solid State Physics, such as the acoustical and the optical phonons and the massless or massive excitations in antiferromagnets. In both examples the dynamics is rather non-trivial at the ultraviolet cutoff. Can we keep such a more unified description of several particles by means of a single quantum field in a renormalizable model? In this case the dynamics at the cutoff can be pushed at infinitely high energies and it is not obvious that the construction converges. Our answer to this question is affirmative up to the one-loop order of the perturbation expansion.

Another interesting aspect of the model considered is the possibility of breaking continuous external symmetries without generating massless Goldstone modes. In fact, suppose that we use say lattice regulator which breaks the continuous translation invariance and the momentum of the condensed particles is close to the cutoff, in which case the continuum description is not applicable at the length scale of the vacuum and there is no reason to expect gapless excitations. This is another manifestation of the apparent homogeneity of the modulated vacuum with shrinking period length.

### III. TREE LEVEL VACUUM

We start the semiclassical solution of our model by determining the minimum of the lattice action. This is in principle a rather involved numerical problem, the minimization of (4). To circumvent this complication we shall seek the tree level, mean-field vacuum in the form

$$\begin{aligned}
\phi_{MF}(x) &= \phi_H + \phi_{IH} \cos \left( K \sum_{\mu=1}^{d_{AF}} x^\mu + \theta \right), \\
K &= 2\pi \frac{M}{N}
\end{aligned} \tag{5}$$

where the amplitudes  $\phi_H$ ,  $\phi_{IH}$ , the relative primes  $N$ ,  $1 \leq M \leq N/2$ , the phase  $\theta$  and the number of the antiferromagnetic directions,  $d_{AF} = 1, 2$  serve as the variational parameters

to minimize the action. We have naturally to confine our study into regions far from the critical points, i.e. above the Ginzburg temperature in order to apply this method. The phase is called para-, ferro-, antiferro- and ferri-magnetic for  $\phi_H = 0 = \phi_{IH}$ ,  $\phi_H \neq 0 = \phi_{IH}$ ,  $\phi_H = 0 \neq \phi_{IH}$  and  $\phi_H \neq 0 \neq \phi_{IH}$ . The action density,  $s(d_{AF}, M, N) = S/L^2$ , on a lattice  $L \times L$  with  $m^2 < 0$  is

$$s_0 = -\frac{m^4}{4\lambda}, \quad (6)$$

for  $d_{AF} = 0$ .

For the computation of the action for  $d_{AF} > 0$  we restrict ourselves to the case  $m^2 < 0$ . The mean-field vacuum configuration is an eigenvector of the lattice box operator,

$$\square\phi_{MF}(x) = -4d_{AF}\sin^2\left(\frac{K}{2}\right)(\phi_{MF}(x) - \phi_H), \quad (7)$$

what gives

$$-\square\mathcal{K}(\square)\phi_{MF}(x) = \mathcal{M}^2(M, N, d_{AF}, c_2, c_4)(\phi_{MF}(x) - \phi_H), \quad (8)$$

with

$$\mathcal{M}^2 = 4d_{AF}\sin^2\left(\frac{K}{2}\right)\left[1 - 4d_{AF}\sin^2\left(\frac{K}{2}\right)c_2 + 16d_{AF}^2\sin^4\left(\frac{K}{2}\right)c_4\right]. \quad (9)$$

The dependence of the eigenvalue  $\mathcal{M}$  in the parameters  $M, N, d_{AF}, c_2, c_4$  will be suppressed in the expressions below. The action density to minimize is

$$s = \frac{m^2}{2}\phi_H^2 + \frac{C_2(N)}{2}(m^2 + \mathcal{M}^2)\phi_{IH}^2 + \lambda\left(\frac{1}{4}\phi_H^4 + \frac{3C_3(N)}{4}\phi_H\phi_{IH}^3 + \frac{3C_2(N)}{2}\phi_H^2\phi_{IH}^2 + \frac{C_4(N)}{4}\phi_{IH}^4\right), \quad (10)$$

where we introduced the notation

$$C_n(N) = \left[\frac{1}{N} \sum_{\ell=1}^N \cos^n\left(2\pi\frac{M\ell}{N} + \theta\right)\right]^{d_{AF}}. \quad (11)$$

Notice the  $M$ -independence of the sum for the relative primes  $M, N$ . Direct computation gives

$$\begin{aligned} C_2(N) &= \begin{cases} \left(\frac{1+\cos 2\theta}{2}\right)^{d_{AF}} & N = 2, \\ 2^{-d_{AF}} & N > 2, \end{cases} \\ C_3(N) &= \begin{cases} \left(\frac{\cos 3\theta}{4}\right)^{d_{AF}} & N = 3, \\ 0 & N \neq 3, \end{cases} \\ C_4(N) &= \begin{cases} \left(\frac{3+4\cos 2\theta+\cos 4\theta}{8}\right)^{d_{AF}} & N = 2, \\ \left(\frac{3+\cos 4\theta}{8}\right)^{d_{AF}} & N = 4, \\ \left(\frac{3}{8}\right)^{d_{AF}} & N = 3 \text{ or } N > 4. \end{cases} \end{aligned} \quad (12)$$

The dependence of  $C_n$  in  $N$  will not be shown explicitly below. One can see from the above construction that the mean-field solution of a model  $\phi^\ell$  requires the coefficients  $C_n$  with  $n = 1, \dots, \ell$ . So the limit  $N \rightarrow \infty$ , the regular dependence on  $N$  sets on for  $N > \ell$ .

The action density corresponding to different choices of  $N$  is obtained as follows:

$N = 2$ : The phase parameter  $\theta$  is redundant in this case. We choose  $\theta = 0$ , what sets  $C_2 = C_4 = 1$ , and write

$$s = A \cdot X + \frac{1}{2} X \cdot B \cdot X, \quad (13)$$

where

$$X = \begin{pmatrix} \phi_H^2 \\ \phi_{IH}^2 \end{pmatrix}, \quad A = \frac{1}{2} \begin{pmatrix} m^2 \\ m^2 + \mathcal{M}^2 \end{pmatrix}, \quad B = \frac{\lambda}{2} \begin{pmatrix} 1 & 3 \\ 3 & 1 \end{pmatrix}. \quad (14)$$

By the help of the shift  $Y = X + X_0$  where

$$X_0 = \frac{1}{8\lambda} \begin{pmatrix} -2m^2 - 3\mathcal{M}^2 \\ -2m^2 + \mathcal{M}^2 \end{pmatrix}. \quad (15)$$

we obtain  $s = \frac{1}{2} Y \cdot B \cdot Y + s_m$ . The rotation matrix

$$\mathcal{R}(\Theta) = \begin{pmatrix} \cos \Theta & \sin \Theta \\ -\sin \Theta & \cos \Theta \end{pmatrix} \quad (16)$$

with  $\Theta = \pi/4$  diagonalizes the quadratic form,

$$s = -\frac{\lambda}{4}(Y^1 - Y^2)^2 + \frac{\lambda}{2}(Y^1 + Y^2)^2 + s_m. \quad (17)$$

The minimum is the result of the competition between the negative and the positive eigenvalue, i.e. the trend to increase  $|Y^1 - Y^2|$  and to decrease  $|Y^1 + Y^2|$ . The result is that the minimum is reached at the boundary of the quadrant  $X^1 \geq 0, X^2 \geq 0$ , i.e. there is no ferrimagnetic phase realized. Thus the mean-field vacuum is found at the minimum of the following two functions

$$s(\phi_H^2, 0) = \frac{1}{2}m^2\phi_H^2 + \frac{\lambda}{4}\phi_H^4, \quad s(0, \phi_{IH}^2) = \frac{1}{2}C_2(m^2 + \mathcal{M}^2)\phi_{IH}^2 + \frac{\lambda}{4}C_4\phi_{IH}^4. \quad (18)$$

The vacuum is antiferromagnetic when

$$\frac{C_2^2}{C_4} \left(1 + \frac{\mathcal{M}^2}{m^2}\right)^2 > 1 \quad (19)$$

with the action density

$$s = s_0 \frac{C_2^2}{C_4} \left(1 + \frac{\mathcal{M}^2}{m^2}\right)^2. \quad (20)$$

$N = 3$ : The minimization of the action with respect  $\theta$  yields the condition  $\phi_H\phi_{IH}^3 \sin 3\theta = 0$ , whose solutions,  $\phi_H = 0, \phi_{IH} = 0$  and  $\theta = 0, \pi/3$  correspond to the anti-, ferro- and

ferrimagnetic phases, respectively. The transformation  $\theta \rightarrow \theta + \pi/3$ , and  $\phi_H \rightarrow -\phi_H$  leaves the mean field action invariant and it is sufficient to consider the case  $\theta = 0$  to explore the ferrimagnetic phase. The action density in the ferro- and antiferromagnetic phases is given by (18) for  $\theta \neq 0$ . The antiferromagnetic phase is preferred for (19) and the corresponding action density is (20). For  $\theta = 0$  we have to minimize (10) numerically.

$N = 4$ : The minimization with respect  $\theta$  yields  $\phi_{IH}^4 \sin 4\theta = 0$ , showing the possibility of the ferrimagnetic phase when  $\theta = n\pi/4$ . Since the action is an even function of the amplitudes  $\phi_H$  and  $\phi_{IH}$  for even  $N$  we have the expression (13) where

$$A = \frac{1}{2} \begin{pmatrix} m^2 \\ C_2(m^2 + \mathcal{M}^2) \end{pmatrix}, \quad B = \frac{\lambda}{2} \begin{pmatrix} 1 & 3C_2 \\ 3C_2 & 1 \end{pmatrix} \quad (21)$$

what results

$$X_0 = \frac{1}{\lambda(9C_2^2 - C_4)} \begin{pmatrix} m^2(1 - 3C_2^2) - 3C_2^2\mathcal{M}^2 \\ m^2C_2(C_4 - 3C_2) + C_2C_4\mathcal{M}^2 \end{pmatrix}. \quad (22)$$

The rotation (16) satisfying the condition  $\cot 2\Theta = (1 - C_4)/6C_2$  transforms the action into the diagonal form with the eigenvalues:

$$\frac{\lambda}{2} \left( 1 + C_4 \pm \sqrt{(1 + C_4)^2 + 36C_2^2 - 4C_4} \right), \quad (23)$$

indicating that one of the normal modes is again unstable. Due to the negative eigenvalue and  $0 < \Theta < \pi/4$ , the minimum is always reached at the boundary of the quadrant  $X^1 \geq 0$ ,  $X^2 \geq 0$ , i.e. there is no ferrimagnetic phase. The condition for the antiferromagnetic phase and the expression of the action density are given by (19) and (20).

$N > 4$ : The procedure is the same as for  $N = 4$ , with the only difference is that  $C_3 = 0$  and there is no  $\theta$ -dependence in the sums  $C_2$  and  $C_4$ .

Phase structure: The resulting action densities are summarized in Table I. The  $c_4$  dependence of the period length of the vacuum for  $c_2 = 2$  and  $N \leq N_{max} = 32$  is shown in Fig. 1. The general trend is that the increase of  $c_4$  pushes the minimum of the dispersion relation  $p_{min}$  towards zero thereby increasing the period length of the vacuum. At a certain threshold value the minimum at  $p_{min}$  becomes so shallow that the potential energy turns the vacuum homogeneous and the system undergoes a ferromagnetic phase transition. Notice the usual signatures of the commensurate-incommensurate transitions, the "devil's staircase" structure. This is a competition between two length scales, the cutoff  $a$  and the period length of the condensate  $\lambda_{vac}$ ,

$$M\lambda_{vac} = Na. \quad (24)$$

The period length in lattice spacing units,  $N(c_2, c_4)/M(c_2, c_4)$  is shown in Fig. 1 as the function of  $c_4$ . It "locks-in", i.e. stays constant in a larger commensurate interval where the relative primes  $N$  and  $M$  are small. The long strips corresponding to the  $N = 2$  and  $4$  phases show a strong "lock-in" effect, contrasted with the gradual change of the period length for other values of  $N$ . The numerator and the denominator as the functions of  $c_4$  are non-monotonic in the same time.

The phase structure in the plane  $(c_2, c_4)$  is depicted in Fig. 2. We identified the mean-field parameters  $N \leq N_{max} = 32$ ,  $M$  and  $d_{AF}$  for each point in the plane  $(c_2, c_4)$ . The

points where we enter into a phase with  $M = 1$  by increasing  $c_4$  are indicated by the solid lines, the other phase boundaries are shown by dotted lines. The increase of  $N_{max}$  makes the dotted lines denser without changing the solid lines or populating the white area. The vacuum in the upper left region is ferromagnetic. The lower right part of the  $c_2, c_4 > 0$  quadrant contains the inhomogeneous vacua, each of them situated in slightly tilted strips with increasing  $N/M$  as we move upwards. The narrow triangular phase between the  $N = 2$  relativistic and non-relativistic phase is a relativistic phase with  $N = 3$ , see Fig. 3. It is interesting that the relativistic vacua are realized for  $N = 2$  and 3 only. We found no ferrimagnetic phase for the parameters considered.

#### IV. EXCITATION BANDS

The study of the more detailed structure of the dynamics starts with the determination of the possible excitations. The distinguishing feature of the antiferromagnetic vacua is their inhomogeneity and the nonconservation of the momentum of the excitations. We introduce in this Section a convenient formalism for the description of the elementary excitations. Following the solid state analogies we rewrite our action by means of the Bloch waves which take the non-conservation of the momentum into account.

Brillouin zones: First we split the first Brillouin zone

$$\mathcal{B} = \{p_\mu; |p_\mu| \leq \pi, \mu = 1, 2\} \quad (25)$$

of the  $d$  dimensional  $N$  antiferromagnetic phase into  $N^{d_{AF}}$  sub-zones within which the Bloch momentum is conserved. In the relativistic case when  $d_{AF} = d$ , we find

$$\mathcal{B}_\alpha^r = \left\{ p_\mu; |p_\mu - P_\mu^{(N)}(\alpha)| \leq \frac{\pi}{N} \right\}, \quad (26)$$

where the center of the sub-zone,  $P_\mu^{(N)}(\alpha)$ , is given by

$$P_\mu^{(N)}(\alpha) = \frac{2\pi}{N} n_\mu(\alpha) \quad (27)$$

in terms of the integer valued vector  $n_\mu(\alpha) = 0, \dots, N - 1$ ,

$$\alpha = 1 + \sum_\mu n_\mu(\alpha) N^{\mu-1}. \quad (28)$$

In other words, the integer component vector  $n_\mu(\alpha)$  gives the center of the sub-zone  $\mathcal{B}_\alpha^r$  in units of  $2\pi/N$ . In the same time, it can be considered as an  $N$ -base number. In this case its value labels the corresponding sub-zones. In the nonrelativistic case,  $d_{AF} < d$ , we have

$$\mathcal{B}_\alpha^{nr} = \left\{ p_\mu; |p_\mu - P_\mu^{(N)}(\alpha)| \leq \frac{\pi}{2}, \mu \leq d_{AF}, |p_\mu| \leq \pi, \mu > d_{AF} \right\}. \quad (29)$$

In the next step we introduce a field variable in real space which is responsible for the fluctuations in each sub-zone,

$$\phi_\alpha(x) = \int_{\mathcal{B}_\alpha} \frac{d^d p}{(2\pi)^d} e^{ip \cdot x} \phi(p) = \int_{\mathcal{B}_1} \frac{d^d \tilde{p}}{(2\pi)^d} e^{i(\tilde{p} + P^{(N)}(\alpha)) \cdot x} \phi_\alpha(\tilde{p}) \quad (30)$$

by the help of the Fourier transform

$$\phi(p) = \frac{1}{L^d} \sum_x e^{-ix \cdot p} \phi(x), \quad (31)$$

and its restriction into the sub-zones,  $\phi_\alpha(\tilde{p}) = \phi(\tilde{p} + P^{(N)}(\alpha))$ . The computation what follows is considerably simplified if the  $N^{d_{AF}}$  Fourier transforms are extended over the first Brillouin zone as periodic functions,

$$\phi_\alpha(\tilde{p}) = \phi_\alpha(\tilde{p} + P^{(N)}(\beta)), \quad (32)$$

where  $\beta$  is an arbitrary sub-zone index. The tilde on a momentum variable will always denote that the given momentum is in the sub-zone  $\mathcal{B}_1$ . The path integral is then written as

$$\prod_p \int d\phi(p) e^{-S[\phi]} = \prod_\alpha \prod_{\tilde{p}} \int \phi_\alpha(\tilde{p}) e^{-S[\phi_\alpha]}, \quad (33)$$

with

$$\begin{aligned} L^d S[\phi_\alpha] = & \frac{1}{2} \int \frac{d^d p}{(2\pi)^d} \phi(-p) [\mathcal{P}^2 \mathcal{K}(-\mathcal{P}^2) + m^2] \phi(p) \\ & + \frac{\lambda}{4} \left( \prod_{k=1}^4 \int \frac{d^d p_k}{(2\pi)^d} \phi(p_k) \right) (2\pi)^d \delta\left(\sum_k p_k\right) \end{aligned} \quad (34)$$

where

$$\mathcal{P}^2(p) = 4 \sum_\mu \sin^2 \frac{p_\mu}{2} \quad (35)$$

denotes the momentum square on the lattice.

Flavor algebra: The  $N^{d_{AF}}$  sub-zones introduced above correspond to the different excitation bands of the coarse grained lattice whose lattice sites represent the primitive cells of the original lattice. The umklapp processes where a non-vanishing momentum is exchanged with the vacuum take the momentum from one sub-zone to another. To separate the sub-zone preserving and changing processes from each other we rewrite the momentum integrals in (34) as a sum over the sub-zones and integration within  $\mathcal{B}_1$ ,

$$\int d^d p f(p) = \sum_{\alpha=1}^{N^{d_{AF}}} \int d^d \tilde{p} f(\tilde{p} + P^{(N)}(\alpha)). \quad (36)$$

The summation can be organized in a more transparent manner by considering the group

$$Z_{d_{AF}, N} = \otimes \prod_{j=1}^{d_{AF}} Z_N \quad (37)$$

which describes the shift of the momentum in the periodic,  $d_{AF}$  dimensional region of the Brillouin zone. This group makes its appearance by considering the action (34) as a matrix element of an operator in the function space span by the "wave functions"  $\phi_\alpha(\tilde{p})$ . It is

advantageous to use the plane wave basis  $|P^{(N)}(\alpha) + \tilde{p}\rangle = |\alpha, \tilde{p}\rangle$  in which the matrix element of the field operator  $\phi_\alpha(\tilde{p})$  is defined by

$$\begin{aligned} \langle \beta', \tilde{q}' | \phi_\alpha(\tilde{p}) | \beta, \tilde{q} \rangle &= \delta \left( P^{(N)}(\beta) + \tilde{q} + P^{(N)}(\alpha) + \tilde{p} - P^{(N)}(\beta') - \tilde{q}' \right) \phi_\alpha(\tilde{p}) \\ &= \delta \left( P^{(N)}(\beta) + P^{(N)}(\alpha) - P^{(N)}(\beta') \right) \delta(\tilde{q} + \tilde{p} - \tilde{q}') \phi_\alpha(\tilde{p}) \\ &= (\gamma^\alpha)_{\beta', \beta} \delta(\tilde{q} + \tilde{p} - \tilde{q}') \phi_\alpha(\tilde{p}), \end{aligned} \quad (38)$$

where the periodicity (32) was used in the second line. The symbol  $\phi_\alpha(\tilde{p})$  stands for operator when sandwiched between the basis vectors and for function in the c-number expressions. We introduced here a representation of  $Z_{d_{AF}, N}$  by means of  $N^{d_{AF}} \times N^{d_{AF}}$  matrices,

$$(\gamma^\alpha)_{\rho, \sigma} = \prod_{\mu=1}^{d_{AF}} \delta_{\sigma_\mu + \alpha_\mu, \rho_\mu (\text{mod } N)}, \quad (39)$$

constructed in such a manner that  $\gamma^\alpha$  describes the effect of the exchange of the momentum  $P^{(N)}(\alpha)$  on the index labeling the sub-Brillouin zones. We shall need later a relation arising from the Abelian nature of the group  $Z_{d_{AF}, N}$ ,

$$(\Gamma)_{\alpha+\rho(\text{mod } N), \beta+\rho(\text{mod } N)} = (\gamma^\rho \Gamma (\gamma^\rho)^{-1})_{\alpha, \beta} = (\Gamma)_{\alpha, \beta}, \quad (40)$$

where  $\Gamma$  is an arbitrary product of the  $\gamma$  matrices. The action can now be rewritten in a more compact notation as

$$L^d S[\phi] = \langle 0, 0 | \frac{1}{2} \phi(0) [\mathcal{P}^2 \mathcal{K}(-\mathcal{P}^2) + m^2] \phi(0) + \frac{\lambda}{4} \phi^4(0) | 0, 0 \rangle \quad (41)$$

where the operator  $\phi(0)$  is given by

$$\phi(0) = \int \frac{d^d p}{(2\pi)^d} \phi(p) = \sum_\alpha \int \frac{d^d \tilde{p}}{(2\pi)^d} \phi_\alpha(\tilde{p}). \quad (42)$$

Elementary rearrangements yield

$$L^d S[\phi] = \text{tr} \left\{ \frac{1}{2} \int \frac{d^d \tilde{p}}{(2\pi)^d} \phi(-\tilde{p}) [\tilde{\mathcal{K}}(\tilde{p}) + \tilde{m}^2] \phi(\tilde{p}) + \frac{\lambda}{4} \left( \prod_{k=1}^4 \int \frac{d^d \tilde{p}_k}{(2\pi)^d} \phi(\tilde{p}_k) \right) (2\pi)^d \delta(\sum_k p_k) \right\}, \quad (43)$$

where  $\phi = \phi_\alpha \gamma^\alpha$ , and the matrices  $\tilde{\mathcal{K}}(\tilde{p})$  and  $\tilde{m}^2$  are given by

$$\begin{aligned} \tilde{\mathcal{K}}_{\alpha, \beta}(\tilde{p}) &= \delta_{\alpha, \beta} \mathcal{P}^2 (P^{(N)}(\alpha) + \tilde{p}) \mathcal{K}(-\mathcal{P}^2 (P^{(N)}(\alpha) + \tilde{p})), \\ \tilde{m}_{\alpha, \beta}^2 &= \delta_{\alpha, \beta} m^2. \end{aligned} \quad (44)$$

The action (43) includes  $N^{d_{AF}}$  fields whose flavor mixing is handled by the matrices  $\gamma_\alpha$ . In fact, the real space expression is

$$S[\phi] = \int d^d x \text{tr} \left\{ \frac{1}{2} \partial_\mu \phi(x) \mathcal{K} \left( \frac{(2\pi)^2}{\Lambda^2} \square \right) \partial_\mu \phi(x) + V(\phi(x)) \right\}. \quad (45)$$

In lattice regularization the lattice sites correspond to the primitive unit cells of the original vacuum. Our goal, to trade the momentum non-conservation on an inhomogeneous vacuum into a multiplicity of excitation bands over a homogeneous vacuum, is completed.

## V. ELEMENTARY EXCITATIONS

We determine in this section the elementary excitations which are the eigenfunctions of the second functional derivative of the action, evaluated at the tree level vacuum. We choose our tree level vacuum in the phase  $N$  to be

$$\phi(x) = \sum_{\alpha} e^{ix \cdot P^{(N)}(\alpha)} \Phi_{\alpha}. \quad (46)$$

We need the eigenvectors of

$$G_{\alpha,\beta}^{-1}(\tilde{p}) = \frac{\delta^2 S[\phi]}{\delta \phi_{\alpha}(-\tilde{p}) \delta \phi_{\beta}(\tilde{p})}_{|\phi=\Phi} = \left( \tilde{\mathcal{K}}(\tilde{p}) + \tilde{m}^2 + 3\lambda\Phi^2 \right)_{\alpha,\beta}. \quad (47)$$

The propagator can formally be written as

$$G(\tilde{p}) = \sum_{\alpha=1}^{N^{d_{AF}}} \psi_{\alpha}(\tilde{p}) \lambda_{\alpha}^{-1}(\tilde{p}) \psi_{\alpha}^{\dagger}(\tilde{p}), \quad (48)$$

where

$$\left( \tilde{\mathcal{K}}(\tilde{p}) + \tilde{m}^2 + 3\lambda\Phi^2 \right) \psi_{\alpha}(\tilde{p}) = \lambda_{\alpha}(\tilde{p}) \psi_{\alpha}(\tilde{p}). \quad (49)$$

The diagonalization of the quadratic part of the action for a given Bloch wave number provides the propagator and the corresponding band structure,  $\lambda_{\alpha}(\tilde{p})$ .

We start with small values of  $c_4$ , i.e. we are either in the ferromagnetic or in the  $N = d_{AF} = 2$  antiferromagnetic phase, when  $\Phi_{\alpha} = \delta_{\alpha,1}\phi_{IH}$ , or  $\Phi_{\alpha} = \delta_{\alpha,4}\phi_{IH}$ , respectively. Since  $\gamma_{\alpha}^2 = 1$  the inverse propagator is

$$G^{-1}(p) = m_{MF}^2 + \hat{p}^2 \mathcal{K}(-\hat{p}^2), \quad (50)$$

where

$$\hat{p}_{\mu} = 2 \sin \frac{p_{\mu}}{2} \quad (51)$$

and

$$m_{MF}^2 = m^2 + 3\lambda\phi_1^2 = \begin{cases} -2m^2 & \text{ferromagnetic,} \\ -2m^2 - 3\mathcal{M}^2(1, 2, d_{AF}, c_2, c_4) & \text{antiferromagnetic.} \end{cases} \quad (52)$$

The propagator can be written as

$$G^{-1} = m_{MF}^2 + \mathcal{P}^2 \left( 1 - c_2 \mathcal{P}^2 + c_4 \mathcal{P}^4 \right), \quad (53)$$

or

$$G_{\alpha,\beta}(\tilde{p}) = \delta_{\alpha,\beta} G(P^{(2)}(\alpha) + \tilde{p}). \quad (54)$$

The long wavelength fluctuations give

$$G_{\alpha,\beta}^{-1}(\tilde{p}) = \delta_{\alpha,\beta} \left[ m_{MF}^2(\alpha) + Z(\alpha)p^2 + O(p^4) \right] \quad (55)$$

where

$$m_{MF}^2(\alpha) = m_{MF}^2 + \mathcal{M}^2(1, 2, n_1(\alpha) + n_2(\alpha), c_2, c_4) \quad (56)$$

and

$$Z(\alpha) = \begin{cases} 1 & \alpha = 1 \\ -1 + 8c_2 - 48c_4 & \alpha = 4 \end{cases} \quad (57)$$

The inverse propagator always has a local minimum at  $\mathcal{P}^2 = 0$ . For certain values of  $c_2$  and  $c_4$  it may develop another minimum at  $\mathcal{P}^2 = \mathcal{P}_r^2 > 0$  when considered as a function of  $\mathcal{P}^2$ . This minimum is realized kinematically for  $\mathcal{P}_r^2 \leq 8$  only, when it is reached on a closed line in the Brillouin zone, c.f. Fig. 6, a structure reminiscent of the roton spectrum [8]. Thus the van der Waals-type force, represented by the choice  $c_2 > 0$  leads directly to the appearance of the additional minima of the dispersion relation interpreted as rotons [9].

To follow this in detail, c.f. Fig. 3, we start with the condition for the extremum,

$$\frac{\partial}{\partial p_\mu} G^{-1}(p) = 2 \sin p_\mu \left( 1 - 2c_2 \mathcal{P}^2 + 3c_4 \mathcal{P}^4 \right). \quad (58)$$

Apart of the points  $p_\mu = P_\mu^{(2)}(\alpha)$  which are always solutions, the root of the expression in the parentheses yields another extremum,

$$\mathcal{P}_r^2 = \frac{c_2}{3c_4} \left( 1 + \sqrt{1 - 3 \frac{c_4}{c_2^2}} \right), \quad (59)$$

so long as

$$c_4 \leq \frac{c_2^2}{3}. \quad (60)$$

The extremum at  $\mathcal{P}^2 = \mathcal{P}_r^2$  is always a minimum. To select the other minima we need the second derivative matrix,

$$\frac{\partial^2 G^{-1}(p)}{\partial p_\mu \partial p_\nu} = 2\delta_{\mu,\nu} \cos p_\mu \left( 1 - 2c_2 \mathcal{P}^2 + 3c_4 \mathcal{P}^4 \right) - 8 \sin p_\mu \sin p_\nu \left( c_2 - 3c_4 \mathcal{P}^2 \right). \quad (61)$$

The sub-zones  $\alpha = 1$  and  $4$  contain particle like excitations because the centers of these sub-zones are local minima,

$$\begin{aligned} \frac{\partial^2}{\partial p_\mu \partial p_\nu} G^{-1}(p)_{|p=P^{(2)}(1)} &= 2\delta_{\mu,\nu} \\ \frac{\partial^2}{\partial p_\mu \partial p_\nu} G^{-1}(p)_{|p=P^{(2)}(4)} &= -2\delta_{\mu,\nu}(1 - 16c_2 + 192c_4). \end{aligned} \quad (62)$$

In contrary, the other sub-zones contain saddle point only and do not support particle like excitations,

$$\begin{aligned}
\frac{\partial^2}{\partial p_1 \partial p_1} G^{-1}(p)_{|p=P^{(2)}(2)} &= -\frac{\partial^2}{\partial p_2 \partial p_2} G^{-1}(p)_{|p=P^{(2)}(2)} \\
&= -\frac{\partial^2}{\partial p_1 \partial p_1} G^{-1}(p)_{|p=P^{(2)}(3)} \\
&= \frac{\partial^2}{\partial p_2 \partial p_2} G^{-1}(p)_{|p=P^{(2)}(3)} \\
&= -2(1 - 8c_2 + 48c_4).
\end{aligned} \tag{63}$$

When  $c_4$  is small enough then  $\mathcal{P}_r^2 > 8$  and the inverse propagator possesses two discrete minima, at  $p = P^{(2)}(1) = (0, 0)$  and at  $p = P^{(2)}(4) = (\pi, \pi)$ . The absolute minimum is at

$$p = \begin{cases} (0, 0) & \text{ferromagnetic,} \\ (\pi, \pi) & \text{antiferromagnetic.} \end{cases} \tag{64}$$

As the value of  $c_4$  is gradually increased from zero  $\mathcal{P}_r^2$  reaches the value 8 and it is better to follow what happens in the two phases separately. In the ferromagnetic phase the degenerate local minima are found along a closed loop in the vicinity of the point  $p = (\pi, \pi)$  when (59) reaches the allowed kinematical regime,  $\mathcal{P}_r^2 < 8$ , for

$$\frac{c_2}{24} < c_4, \quad \text{and} \quad \frac{c_2}{12} - \frac{1}{192} < c_4. \tag{65}$$

This line becomes the absolute minimum when the smaller root of the expression

$$1 - c_2 \mathcal{P}^2 + c_4 \mathcal{P}^4 \tag{66}$$

as the function of  $\mathcal{P}^2$  turns out to be smaller than 8,

$$\frac{c_2}{16} < c_4 \quad \text{or} \quad c_4 < \frac{c_2}{8} - \frac{1}{64}. \tag{67}$$

In fact, (66) is negative between the roots and the inverse propagator goes below its value at  $\mathcal{P}^2 = 0$  according to (53).

It is shown in Fig. 3 that the line of degenerate local minima appears within the region bounded by the part ab of the parabola P, (60) and the line segments bc and ac, defined by the first and the second inequalities of (67) and (65), respectively. The line of degenerate minima turns out to be absolute minimum below the parabola (60) and above the line segment bc and the ferro- antiferromagnetic phase boundary. The absolute minimum of the inverse propagator is degenerate and lies on a closed line in either phase for  $c_2 > 1/4$  when the inequality (67) is trivially satisfied.

As the value of  $c_4$  is increased in the antiferromagnetic phase the inverse propagator keeps its minimum at  $p = (\pi, \pi)$  so long as the second inequality of (65) is violated. The absolute minimum is degenerate and found along a closed loop around  $p = (\pi, \pi)$  when  $c_4$  is further increased. We may avoid the phase  $N = 3$  by choosing large enough  $c_2$  and arrive at the  $N = 2$  nonrelativistic phase without modifying the propagator at the phase transition. The value of the lattice momentum at the minimum, (59), is a monotonically decreasing function of  $c_4$  and reaches 4 for

$$c_4 = \frac{c_2}{6} - \frac{1}{48}, \quad (68)$$

the line S of Fig. 3. At this point the degenerate minima of the inverse propagator form a square and for larger values of  $c_4$  it is deformed into a closed loop around  $p = 0$ .

The further increase of  $c_4$  brings us to the higher  $N$  phase boundaries and the situation becomes more involved.

We turn now to the question of the critical points. According to (52) and (56) the second order phase transition is reached when both  $m^2 \rightarrow 0$  and  $\mathcal{M}^2 \rightarrow 0$  for  $m^2 < 0$ . Let us take

$$\mathcal{M}^2 = -\mu_{\mathcal{M}}^2 a^2, \quad m^2 = -\mu_m^2 a^2. \quad (69)$$

The first equation and (9) assert that the criticality is reached either for

$$c_4 \approx \frac{c_2}{4d_{AF} \sin^2\left(\frac{K}{2}\right)} - \frac{1}{16d_{AF}^2 \sin^4\left(\frac{K}{2}\right)}, \quad (70)$$

or as  $N/M \rightarrow \infty$ . Both cases require the vicinity of the ferro- antiferromagnetic transition line, the value of  $c_2$  and  $c_4$  is finite in the first case and diverging in the second. Since  $C_4(N) \geq C_2^2(N)$  (20) shows that  $\mu_{\mathcal{M}}^2 > 0$  is needed to reach this phase transition. Thus the ferro-antiferromagnetic transition line is critical in the mean-field approximation.

We close this Section with a remark about the Goldstone modes. The inhomogeneous vacuum breaks the external symmetries and we find Goldstone modes for the models in the continuum. The lattice regulator reduces the space-time symmetries into a discrete group and there is no reason to expect massless phonons in the antiferromagnetic phases. But the strength of the breaking of the continuous part of the space-time symmetries is  $O(M/N)$ . Thus the continuous kinematical symmetries are restored as  $N/M \rightarrow \infty$  and the Goldstone theorem is regained asymptotically, i.e.  $\lambda(p_{min}) = O(M/N)$ . An important consequence of this gradual restoration of the Goldstone theorem is the absence of long range modes and the possibility of supporting the periodic vacuum in two dimensions when  $N$  is finite. This does not mean a long range order because the non-trivial part of the vacuum is squeezed within the distance  $Na/M \rightarrow 0$ .

## VI. ONE-LOOP RENORMALIZATION

It is shown in this Section that the one-loop effective potential of our model can be made finite by the introduction of an appropriate mass counterterm and the ferro-antiferromagnetic transition remains a critical line on the one-loop level.

It is straightforward to derive the Feynman rules for (43) and to compute the radiative corrections. The one-loop effective potential, the generating function for the 1PI vertices,

$$V_{eff}(\Phi) = \sum_{n=0}^{\infty} \frac{1}{n!} \sum_{\alpha_1, \dots, \alpha_n} \Phi_{\alpha_1} \dots \Phi_{\alpha_n} \Gamma^{(n)}(P^{(N)}(\alpha_1), \dots, P^{(N)}(\alpha_n)), \quad (71)$$

can be written in the one-loop approximation as

$$V_{eff}(\Phi) = V_{tree}(\Phi) + \frac{1}{2} \int \frac{d^d \tilde{p}}{(2\pi)^d} \text{tr} \ln [\tilde{\mathcal{K}}(\tilde{p}) + \tilde{m}^2 + 3\lambda\Phi^2], \quad (72)$$

where

$$V_{tree}(\Phi) = \text{tr} \left( \frac{1}{2} \tilde{\mathcal{K}}(0) \Phi^2 + \frac{1}{2} m^2 \Phi^2 + \frac{\lambda}{4} \Phi^4 \right). \quad (73)$$

We split the mass term into a renormalized and a counterterm,

$$m^2 = m_R^2 + \delta m^2, \quad (74)$$

and make the replacement  $m^2 \rightarrow m_R^2$  in the loop integral.

The  $\Phi$ -dependence of the one-loop integrals can significantly be simplified by using the relation (40) with  $\Gamma = \Phi^2$ ,

$$(\Phi^2)_{\alpha,\alpha} = \frac{1}{N^{d_{AF}}} \text{tr} \Phi^2, \quad (75)$$

where no summation is made for the index  $\alpha$ . Since the matrix  $\tilde{K}(\tilde{p}) + \tilde{m}_R^2$  is diagonal,

$$V_{eff}(\Phi) = V_{tree}(\Phi) + \frac{1}{2} \int \frac{d^d \tilde{p}}{(2\pi)^d} \text{tr} \ln \left[ \tilde{\mathcal{K}}(\tilde{p}) + \tilde{m}_R^2 + \frac{3\lambda}{N^{d_{AF}}} \text{tr}(\Phi^2) \right]. \quad (76)$$

The ultraviolet divergences are identified in two steps. First we expand in the field dependence and write the loop contribution as

$$\sum_n \frac{1}{2n} \int \frac{d^d \tilde{p}}{(2\pi)^d} \text{tr} \left( \frac{3\lambda \text{tr} \Phi^2}{\tilde{\mathcal{K}}(\tilde{p}) + \tilde{m}_R^2} \right)^n, \quad (77)$$

to recover the usual one-loop resummation in the effective potential. In the second step we expand the integrals in the lattice spacing  $a$ ,

$$a^{2n-d} \int_{|p|<\pi/N} \frac{d^d \tilde{p}}{(2\pi)^d} \text{tr} \left( \tilde{\mathcal{K}}(\tilde{p}) + \tilde{m}_R^2 \right)^{-n} = \int_{|p|<\pi/Na} \frac{d^d \tilde{p}}{(2\pi)^d} \left[ \sum_{\alpha} \frac{1}{a^2} \mathcal{P}^2 \left( a^2 (P^{(N)}(\alpha) + \tilde{p}) \right) \right. \\ \left. \times K \left( -\frac{1}{a^2} \mathcal{P}^2 \left( a^2 (P^{(N)}(\alpha) + \tilde{p}) \right) \right) + \frac{\tilde{m}_R^2}{a^2} \right]^{-n}. \quad (78)$$

We have at most a logarithmic divergence in two dimensions ( $n = 1$ ) and the dimensionless inverse propagator, the integrand of the left hand side, has a finite,  $1/a$  independent minimum. Let us write the smallest eigenvalue of the inverse propagator around its minimum as

$$\lambda_{\alpha_{min}}(\tilde{p}_{min} + \tilde{p}) = m_4^2 + Z_0 \tilde{p}^2 + O(a^2 \tilde{p}^4), \quad (79)$$

with  $m_0^2 = a^2 m_{min}^2$ , what allows us to identify the divergent part of the loop integral for  $d = 2$ ,

$$\frac{1}{2} \int_{|p|<\pi/Na} \frac{d^2 \tilde{p}}{(2\pi)^2} \frac{1}{m_{min}^2 + Z_0 \tilde{p}^2}. \quad (80)$$

Thus the one loop ultraviolet divergence can be removed by setting

$$\delta m^2 = - \int_{|p| < \pi/Na} \frac{d^2 \tilde{p}}{(2\pi)^2} \frac{1}{m_{min}^2 + Z_0 \tilde{p}^2}. \quad (81)$$

When  $m_{min}^2 = O(a^{-\epsilon})$ ,  $\epsilon > 0$ , then no divergency arises. If there are several finite minima of the dimensionless inverse propagator then we sum over them in the counterterm.

The continuum limit, (69) can be achieved along the ferro-antiferromagnetic transition line of the plane  $(c_2, c_4)$ . We have one or two particles by approaching this line from the ferro- or the antiferromagnetic phase below the point  $c = (1/4, 1/64)$ , respectively. Above the point  $c$  the rotons appear in both phases and replace one of the particles of the antiferromagnetic vacuum. One can find specially interesting continuum limits in the vicinity of the point  $c$ . (i) Approach from below the line  $ab$  in the ferromagnetic phase, which gives a single particle and monotonically increasing inverse propagator with the momentum. (ii) The approach above the line  $ab$  but below  $bc$  yields one particle and rotons. The roton momentum diverges with the cutoff, a reminiscent of the new excitation bands in the antiferromagnetic phase. The value of the inverse propagator at the degenerate minima, the roton mass square is finite but larger than for the absolute minimum, at  $p = 0$ . Thus the rotons are heavier than the particle. (iii) Approaching above the line  $bc$  yields a model with a particle and rotons where the rotons are lighter than the particle. (iv) The approach from the antiferromagnetic phase produces a model with two particles.

## VII. NON-PERTURBATIVE VACUUM

In order to assess the importance of the fluctuations, we performed a Monte Carlo simulation of the model (4). The resulting phase structure is summarized on Fig. 4. The coupling constants  $\lambda = 0.05$ ,  $m^2 = -0.1$  were chosen and the simulation on the line  $c_2 = 2$  was done at  $200 \times 200$  lattice size. The  $c_4$  dependence of the results was monitored with a particular care by scanning the region  $0 \leq c_4 \leq 1$  with step size  $\Delta c_4 = 0.01$ . The other points were obtained on  $40 \times 40$  lattice. The performed tests have showed no appreciable finite size dependence in the qualitative and quantitative features of the phase diagram. We used the metropolis update algorithm, carefully checking the statistics to make sure that no statistical error would change our conclusions concerning the phase diagram. In order to test ergodicity, local cluster algorithms were tried as well as different initial conditions.

The letters along the vertical lines of Fig. 4 indicate the qualitative space-time structure of the vacuum seen in the simulation: A=ordered ( $N = d_{AF} = 2$ ) antiferromagnetic; L=labyrinths; W=plane waves; P=weakly antiferromagnetic (onset of the crossover on the finite lattice), F=ferromagnetic and F'=weakly ferromagnetic. To understand the phase structure we recall that the parameters of the bare action characterize the dynamics at the cutoff. Consequently one may extract useful informations about the short range order of the vacuum by considering the coefficients appearing in the quadratic part of (4). The sign of the coefficients determines the ferro- or antiferromagnetic nature of the couplings. We introduce the subscript  $(n, m)$  which shows the separation of the two field variables multiplied by the given parameter,  $A_{0,0} = 2 + m^2/2 - 10c_2 + 56c_4$ ,  $B_{1,0} = -1 + 8c_2 - 57c_4$ ,  $C_{2,0} = -c_2 + 12c_4$ ,  $E_{1,1} = -2c_2 + 24c_4$ ,  $D_{3,0} = -c_4$  and  $F_{1,2} = -3c_4$ . The lines where  $A$ ,  $B$ ,  $C$  and  $E$  change sign,

$$\begin{aligned}
c_4 &= \frac{10}{56}c_2 - \frac{m^2}{112} - \frac{2}{56} \quad (A), \\
c_4 &= \frac{8}{57}c_2 - \frac{1}{57} \quad (B), \\
c_4 &= \frac{1}{12}c_2 \quad (C, E)
\end{aligned} \tag{82}$$

are shown in Fig. 4 by solid lines. These lines intersect and the short range order varies in a complicated manner for  $c_2 < 0.45$ . But once this value is reached, the sequence of the change of the signs as  $c_4$  increases is always the same. The importance of these signs is that they create frustrations whenever  $c_4 > 0$ . There are no frustration when  $c_4 = 0$  because  $D_{3,0} = F_{2,1} = 0$  and all others favor the  $N = 2$ ,  $d_{AF} = 2$  antiferromagnetic or the ferromagnetic vacuum for  $c_2 > 1/8$  or  $c_2 < 1/8$ , respectively. For  $c_4 > 0$  but below the line  $C, E$ , in the antiferromagnetic  $N = 2$ ,  $d_{AF} = 2$  phase  $B_{1,0} > 0$ ,  $C_{2,0}$ ,  $E_{1,1} < 0$  favor this kind of vacuum. But the other signs,  $D_{3,0}$ ,  $F_{2,1} < 0$  introduce frustrations whose density increases with  $c_4$ . The further increase of  $c_4$  flips the sign of  $B$  and ultimately  $A$ , destabilizes the lock-in mechanism at  $N = 2$  and opens the way for the rapid variations of the devil's staircase. In between the lines  $C, E$  and  $B$ ,  $C_{2,0}$ ,  $E_{1,1} > 0$  and the frustration density is increased because only  $B_{1,0}$  favors this vacuum. The result is a strong increase of the fluctuations. The mean-field approximation is obviously unreliable in this regime and the simulation produces labyrinth-like vacuum, see below. For large  $c_4$ , in the ferromagnetic phase  $B_{1,0}$ ,  $D_{3,0}$ ,  $F_{1,2} < 0$  act in favor of the homogeneous vacuum but  $C_{2,0}$ ,  $E_{1,1} > 0$  generate frustrations which might explain the weakening of the ferromagnetic condensate for large  $c_4$ . For the intermediate values of  $c_4$  the competition between the different terms is more involved and the compromise between the different competing terms is reached over a longer length scale according to the mean-field solution. The qualitative conclusion is the separation of the stable low  $c_4$   $N = 2$ ,  $d_{AF} = 2$  vacuum from the high  $c_4$  ferromagnetic and an intermediate  $c_4$  strongly frustrated antiferromagnetic vacuua.

The frustrations are the lattice defects of the antiferromagnetic vacuum. In order to understand their production mechanism in the  $N = 2$  antiferromagnetic phase we used two different initial conditions, an ordered and a disordered one,

$$\phi_{init}^{ord}(x) = \phi_{IH}(-1)^{x^1+x^2}, \tag{83}$$

and

$$\phi_{init}^{dis}(x) = 0, \tag{84}$$

respectively. The initial condition  $\phi_{init(x)}^{dis}$  which actually looks ordered becomes disordered after few Monte-Carlo sweeps. This happens because it represents an unstable equilibrium position and the local field variable "rolls down" to one of the potential minima  $\phi(x) = \pm\phi_{IH}$ . This leads to the formation of  $N = 2$  antiferromagnetic domain structure. These domains are separated by walls of links where the field variable has the same sign. The region on the plane  $(c_2, c_4)$  where the antiferromagnetic domains consisting of the patches  $\phi_{init}^{ord}(x)$  and  $-\phi_{init}^{ord}(x)$  develop long and winding boundaries is called labyrinth-like and is denoted by L in Fig. 4.

For large values of  $c_2$  the amplitude of the modulated vacuum is large so the frustrations move very slowly in the simulation time. The antiferromagnetic domain walls turned out

to be very slow variables, as well. The domain walls were always generated below the line  $C, E$  of Fig. 4 when the disordered initial configuration was used. The vacuum obtained by the runs with ordered initial configuration did not support the domains. The question is whether the domain walls are real degrees of freedom or reflect the insufficient convergence of the simulation method. We have developed cluster algorithm and found that for small  $c_2$ , ( $c_2 < 1.0$ ), the walls have dynamics, reach an equilibrium and may disappear. For larger  $c_2$  the domain wall motion slows down despite of the cluster algorithm. The thermalization was safely reached within each domain. It remains an intriguing question if the domain walls thermalize in this regime with extremely long relaxation time, i.e we are in a glassy regime [10] or the ergodicity is definitely lost and the vacuum consists of a stable, disordered network of domain walls. In this regime the frustrations act as scattering centers without feedback from the fast dynamics of the elementary excitations, a dynamical situation reminiscent of the quenched disorder in solids. For  $c_2 < 1$  the mean field value,  $\phi_{IH}$ , is small enough to make the domain wall fluctuations more likely and the cluster update averages over the different rearrangements of the domains.

The different regions shown in Fig. 4 were studied in more detail at  $c_2 = 2$ . The negative action density obtained by starting at  $c_4 = 0$  and sweeping the interval  $0 \leq c_4 \leq 1$  is plotted in Fig. 5(a). The results obtained by the ordered and disordered initial configuration are indicated by + and squares, respectively. The ordered vacuum has lower action density up to  $c_4 \approx 0.2$ . The mean-field action density is shown by a solid line. It is instructive to follow the second lowest mean-field solution, indicated by the circles. The splitting between the lowest and the second lowest mean field action level reflects the stability of the vacuum against the change of the long range order. The agreement between the Monte Carlo and the mean-field results is remarkable for small  $c_4$  in the relativistic phase. Right at the relativistic-non relativistic phase transition, the ordered configuration is a rather poor approximation and the disordered vacuum adjusts itself easier to the value  $d_{AF} = 1$ . For  $c_4 > 0.3$  the mean field badly over estimates the true vacuum action density, indicating the presence of strong fluctuations. Notice that the phases with  $N = 2$  and 4 are more stable against the modification of the long range, in agreement with their stronger "lock-in" in Fig. 1.

Another insight into the vacuum can be gained from the inspection of the period length of the vacuum,  $\lambda_{vac}$ , measured by

$$-\frac{\langle \phi \square \phi \rangle}{\langle \phi^2 \rangle} \approx 4d_{AF} \sin^2 \left( \frac{\pi}{\lambda_{vac}} \right). \quad (85)$$

The numerical and the analytical results depicted in Fig. 5(b) show that the first order transitions of the mean field approximation between the relativistic and the non-relativistic  $N = 2$  antiferromagnetic phase is smoothed out in the simulations when the disordered initial condition is used. The ordered initial condition follows the mean field curve within the phase  $N = d_{AF} = 2$ . The slightly higher action of the disordered initial configuration runs indicates that the true vacuum is close to being ordered and the relativistic-non relativistic phase transition is of strongly first order. One is tempted to conclude that the fluctuations smoothen out the commensurate-incommensurate transitions but better statistics is needed to settle this question in a satisfactory manner for the whole phase diagram. The difference between the numerical results and the mean-field solution is the largest in the phase  $N = 2, d_{AF} = 1$ . The mean-field approximation slightly underestimates the period length of the

vacuum in the vicinity of the ferromagnetic transition. This is consistent with one of the remarks made about Fig. 5(a), namely that the fluctuations in this regime are stronger than expected by the mean-field approximation. In fact, the stronger fluctuations lower the critical value of  $c_4$  so the period length of the vacuum diverges faster in function of  $c_4$  than in the mean-field expression.

The strength of the modulation of the vacuum is displayed in Fig. 5(c). It is simplest to express it in terms of the Fourier transformed field

$$\tilde{\phi}(p) = \frac{1}{L^2} \sum_x \phi(x) e^{-ip \cdot x}, \quad (86)$$

obtained on an  $L \times L$  lattice. We may split the expectation value  $\langle |\tilde{\phi}(p)|^2 \rangle$  into the sum of the condensate and the fluctuations,

$$\langle |\tilde{\phi}(p)|^2 \rangle = \langle |\tilde{\phi}(p)|^2 \rangle_c + \langle |\tilde{\phi}(p)|^2 \rangle_{fl}, \quad (87)$$

$$\langle |\tilde{\phi}(p)|^2 \rangle_c = | \langle \tilde{\phi}(p) \rangle |^2, \quad \langle |\tilde{\phi}(p)|^2 \rangle_{fl} = G_c(p). \quad (88)$$

where  $G_c(p)$  stands for the connected propagator, given by (53) in the leading order of the perturbation expansion. A simple approximation for the strength of the modulation of the vacuum is

$$\phi_c^2 = \max_p \langle |\tilde{\phi}(p)|^2 \rangle_c \approx \max_p \langle |\tilde{\phi}(p)|^2 \rangle \approx \langle \max_x \phi(x) \rangle^2 \approx \langle \min_x \phi(x) \rangle^2. \quad (89)$$

$\max_p \langle |\tilde{\phi}(p)|^2 \rangle$  is displayed by plus and square for the ordered and disordered initial configuration, respectively. The star shows the value of the last two expressions in (89). We find that the different estimates for the strength of the condensate agree in the relativistic phase except the simulation results corresponding to the disordered start. The difference between the mean-field solution indicated with x and the numerical results can be considered as a measure of the strength of the fluctuations. Note the local maximum and minimum in the fluctuations at  $c_4 \approx 0.35$  and  $c_4 \approx 0.6$ , respectively. The former is in agreement with the remark made for Fig. 5(b). The average of the extrema of the field in the real space is higher than the mean field value and shows no structure as the function of  $c_4$  indicating that the fluctuations tend to lower the local values of the field variable  $|\phi(x)|$ . As noted before, the fluctuations increase as the ferromagnetic phase is approached, a result consistent with the second order nature of the ferromagnetic phase transition.

The numerical results for the complete propagator, (87) what displays the structure of the vacuum and the elementary excitations in the same time are presented in Fig. 6. We divided the interval  $[0, \max_p \langle |\tilde{\phi}(p)|^2 \rangle]$  into five equal segments and their contourplots are shown in the figures. The strength of the contour line increases with the amplitude, so the blacker regions of the plots indicate the location of the maxima.

$0 < c_4 < 0.16$ : When  $c_4$  is small we are in the relativistic  $N = 2$  phase and  $\langle |\tilde{\phi}(p)|^2 \rangle$  depends strongly on the initial condition of the Monte Carlo simulation. The ordered initial configuration (83) yields a single peak for  $\langle |\tilde{\phi}(p)|^2 \rangle$  at  $p = P^{(2)}(4) = (\pi, \pi)$  suggesting little disorder. In the case of the disordered initial configuration,  $\phi_{init}^{dis}$ , one finds a domain structure and the Fourier transform  $| \langle \tilde{\phi}(p) \rangle |^2$  shown in Fig. 6(a) at  $c_4 = 0$  is depleted at

$p = P^{(2)}(4)$ ,  $\langle |\phi(P^{(2)}(4))|^2 \rangle \approx 0$ , and develops a ring of maxima around this momentum. It is easy to understand the minimum at the center. In fact, assuming that the vacuum consists of the domains of  $\phi_{init}^{ord}(x)$  and  $-\phi_{init}^{ord}(x)$  in the fractions  $c$  and  $1 - c$  of the volume, respectively one finds  $\phi_{cond}^2 = \phi_{IH}^2(1 - 2c)^2/4$ . The domain pattern develops after few sweeps and the domain walls turn out to be rather slow variables.

$0.16 < c_4 < 0.22$ : The excitations become more involved in this regime. The coefficients  $C$  and  $E$  of the lattice action are positive for  $c_4 > 1/6$  making the frustration density higher. Furthermore the propagator develops a circle of degenerate maxima around the point  $p = P^{(2)}(4)$  for  $c_4 > 31/192 \approx 0.16$ . The result is a cusp in the condensate as the function of  $c_4$  cf. Fig. 5(c), and the softening of the modes giving an increase of  $\langle |\tilde{\phi}(p)|^2 \rangle$ .

$0.22 < c_4 < 0.3$ : The ordered initial configuration simulation recovers the right vacuum at  $c_4 \approx 0.23$  in a discontinuous manner, c. f. Fig. 6(b) and (c). For  $c_4 > 0.23$  the simulations corresponding to the two different initial conditions yield the same result. The hysteresis in the  $c_4$  dependence, i.e. the later appearance of the ring for the ordered initial configuration case compared with the unstable starts suggests that the transition  $d_{AF} : 1 \longleftrightarrow 2$  is of first order. The roton minimum in the dispersion relation tends to break the straight lines where the frustrations are found and to distribute them in a more spherically symmetrical manner, resulting in more disorder and creating a labyrinth structure instead of the ordered nonrelativistic antiferromagnetic vacuum.

$0.3 < c_4 < 0.38$ : The minimum of (53) is the longest, being a square, for  $c_4 = 0.31$  according to (68). A typical example shown in Fig. 6(d) witnesses that the fluctuations are the strongest in this regime, when the volume of the phase space occupied by the soft modes is the largest. As the length of the roton minima starts to shrink for  $c_4 > 0.31$  so does the strength of the fluctuations as seen in Fig. 5(c).

$0.38 < c_4 < 0.6$ : The period length of the vacuum growths beyond 2 at  $c_4 \approx 0.38$  and  $\langle |\tilde{\phi}(p)|^2 \rangle$  becomes strongly suppressed at  $p = (0, \pi)$  and  $p = (\pi, 0)$  according to Fig. 6(e)-(f). The rapid variation in  $c_4$  supports the discontinuous nature of the transition  $N = 2 \rightarrow 3$ . The further increase of  $c_4$  makes the restoration of the rotational symmetry more difficult. This is because the symmetry restoration is achieved by forming domains where the plane wave modulation of the vacuum has different orientation. The longer period length of the vacuum makes more energy consuming to break the straight plane wave by changing its direction, i.e. the domain wall energy density increases. This explains the breaking up of the ring into smaller segments and its ultimate reduction to few discrete peaks, as demonstrated in Fig. 6(g).

$c_4 \approx 0.6$ : The fluctuations reach a minimum in the middle of the "lock-in" interval  $N/M = 4$  seen in Fig. 1. The point where  $N/M$  is approximately the power of the highest order terms in the field variable of the lagrangian the above mentioned decrease of the fluctuations comes to a halt and is turned into an opposite trend due to the approach of the ferromagnetic phase transition. In fact, as the length of the roton minima shrinks and becomes less important the increase of  $c_4$  ultimately leads to the disappearance of the condensate which is triggered by the increase of the fluctuations. This is due to a tree-level effect,  $c_4$  makes the modulation of the vacuum more energetic so the amplitude of the modulation decreases with the increase of  $c_4$ . As the amplitude decreases it becomes easier to break a plan wave into domains what amounts to the attempt for the restoration of the rotational symmetry. The maximum in  $\langle |\tilde{\phi}(p)|^2 \rangle$  spreads from a well localized point over

the whole circle of the rotons as  $c_4$  is increased beyond 0.6.

$0.6 < c_4 < 0.98$ : As  $c_4$  increases and  $p_{min}$  approaches zero the dominant fluctuations are grouped on a circle around  $p = 0$  with increasing strength as shown in Fig. 6(h). The condensate weakens and increasing period length in lattice spacing units is in agreement with the one-loop renormalizability established in the previous section.

$c_4 \approx 0.98$ : The precursor of the transition to the ferromagnetic phase is the appearance of a peak in  $\langle |\tilde{\phi}(p)|^2 \rangle$  at  $p = 0$  for  $c_4 \approx 0.98$ . The further increase of  $c_4$  brings us into the ferromagnetic phase with roton excitations.

### VIII. CONCLUSIONS

A simple two dimensional effective theory was considered in this work for an elementary interaction which is strongly repulsive for short distances and attractive at long distances and supposed to form a crystalline ground state. Such an interaction is coded in terms of the effective action with higher order of the derivatives. The inhomogeneous ground state is reproduced in the saddle point approximation of the effective theory.

The mean-field, tree level phase structure of the model is quite involved and displays several inhomogeneous phases with a number of commensurate-incommensurate transitions. The elementary excitations contain modes similar to the rotons of liquid  $He^4$  but the excitation spectrum is usually massive in lacking of a conserved particle number. Our effective theory is a simplified version of the higher dimensional systems with inhomogeneous ground states, such as the solids, antiferromagnets and materials with charge density phase. The formation of the inhomogeneous vacuum by the condensation of particles with non-vanishing momentum is a manifestation of the additional soft modes which characterizes the quantum phase transitions.

The one-loop corrections give a line of ultraviolet fixed points with variable particle content. The period length of the vacuum can thus be sent to zero. The Poincare symmetry is restored in the continuum limit and the vacuum becomes homogeneous for the measurements made at finite energies. In the same time the excitation spectrum of the model remains nontrivial, reflecting the inhomogeneity of the vacuum. The different dispersion relation branches are interpreted in the continuum limit as excitations with different flavor. This unusual vacuum-excitations correspondence opens the way for the construction of new kind of unified quantum field theoretical models where several particles are described by the same field.

The numerical analysis performed by the Monte Carlo method confirms the mean-field prediction of the phase structure and is consistent with the criticality at the ferromagnetic phase transition line. The frustrations are the slow modes of the simulation when the amplitude of the modulated vacuum is large suggesting the possibility of a quenched disorder variable in real time, as well.

We note finally that there are no massless excitation modes above the modulated vacuum with finite period length in lattice spacing units. This is specially striking in two dimensions where the periodic structure of the periodic vacuum is not necessarily destroyed by the Mermin-Wagner-Coleman theorem [12]. The continuum limit of the antiferromagnetic phase where  $N/M \rightarrow \infty$  might be similar to the planar X-Y model with power like decay of the correlations.

## **IX. ACKNOWLEDGEMENT**

We thank Vincenzo Branchina for useful discussions during this work.

## REFERENCES

- [1] V. A. Alessandrini, H. de Vega, F. Schaposnik, *Phys. Rev. B* **10**, 3906 (1974); *Phys. Rev. B* **12**, 5034 (1975); T. Appelquist, J. Carazzone, *Phys. Rev. D* **11**, 2865 (1975); T. Appelquist, J. Carazzone, H. Kluberg-Stern, M. Roth, *Phys. Rev. Lett.* **36**, 768 (1976), *Phys. Rev. Lett.* **36**, 1161 (1976); T. Appelquist, J. Carazzone, *Nucl. Phys. B* **120**, 77 (1977).
- [2] G. Gallavotti, V. Rivasseau, *PLB* **122**, 268 (1983).
- [3] G. Kohring, R. E. Shrock, *Nucl. Phys. B* **295**, 36 (1988); S. Caracciolo, R. G. Edwards, A. Pelissetto, A. D. Sokal, *Nucl. Phys. B Proc. Suppl.* **30**, 815 (1993); J. L. Alonso, A. Tarancón, H. G. Ballesteros, L. A. Fernandez, V. Martin-Mayor, A. Munoz Sudupe, *Phys. Rev. B* **53**, 2537 (1996); M. L. Plummer, A. Caille, *J. Appl. Phys.* **70**, 5961 (1991); H. Kawamura, *J. Phys. Soc. Jpn.* **61**, 1299 (1992); H. G. Ballesteros, L. A. Fernandez, V. Martin-Mayor, A. Munoz Sudupe, *Phys. Lett. B* **378**, 207 (1996); *Nucl. Phys. B* **483**, 707 (1997); P. Azaira, B. Delamotte, T. Jolicoeur, *Phys. Rev. Lett.* **3175**, 1990 ( ); P. Azaira, B. Delamotte, F. Delduc, T. Jolicoeur, *Nucl. Phys. B* **408**, 485 (1993).
- [4] J. L. Alonso, J. M. Carmona, J. Clemente Gallardo, L. A. Fernandez, D. Iniguez, A. Tarancón, C. L. Ullod, *Phys. Lett. B* **376**, 148 (1996); I. Campos, L. A. Fernandez, A. Tarancón, *Phys. Rev. D* **55**, 2965 (1997); H. G. Ballesteros, J. M. Carmona, L. A. Fernandez, V. Martin-Mayor, A. Munoz Sudupe, A. Tarancón, *Phys. Rev. D* **55**, 5067 (1997); Y. Shamir, hep-lat/9512019; J. Fingberg, J. Polonyi, *Nucl. Phys. B* **486**, 315 (1997).
- [5] V. Branchina, H. Mohrbach, J. Polonyi, "The antiferromagnetic  $\phi^4$  model", submitted to *Phys. Rev.*
- [6] M. Fujimoto, *The Physics of Structural Phase Transitions*, Springer, 1997.
- [7] Gy. Grüner, *Density Waves in Solids*, Addison-Wesley, 1994.
- [8] L. D. Landau, E. M. Lifsic, *Theoretical Physics*, vol. IX; Pergamon Press.; R. P. Feynman, M. Cohen, *Phys. Rev.* **107**, 13 (1957).
- [9] R. Feynman, *Phys. Rev.* **91**, 1301 (1953); *Phys. Rev.* **94**, 262 (1954); in *Progress in Low Temperature Physics*, vol I, C. J. Gorter (ed.), North-Holland, 1955.
- [10] K. H. Fischer, J. A. Hertz, *Spin Glasses*, Cambridge University Press, 1991.
- [11] T. R. Kirkpatrick, D. Belitz, "Quantum phase transitions in electronic systems", cond-mat/9707001.
- [12] N. D. Mermin, H. Wagner, *Phys. Rev. Lett.* **17**, 1133 (1966); S. Coleman, *Commun. Math. Phys.* **31**, 259 (1973).

## TABLES

	$d_{AF} = 1$	$d_{AF} = 2$	
$N = 2$	$\left(1 + \frac{4(1-4c_2+16c_4)}{m^2}\right)^2$	$\left(1 + \frac{8(1-8c_2+64c_4)}{m^2}\right)^2$	
$N = 3$	$\frac{2}{3} \left(1 + \frac{3(1-3c_2+9c_4)}{m^2}\right)^2$	$\frac{4}{9} \left(1 + \frac{6(1-6c_2+36c_4)}{m^2}\right)^2$	
$N = 4$	$(1 + 2(1 - 2c_2)^2$	$\left(1 + \frac{4(1-4c_2+16c_4)}{m^2}\right)^2$	
$N > 4$	$\frac{2}{3} \left(1 + \frac{4s^2(1-4s^2c_2+16s^4c_4)}{m^2}\right)^2$	$\frac{4}{9} \left(1 + \frac{8s^2(1-8s^2c_2+64s^4c_4)}{m^2}\right)^2$	

TABLE I. The antiferromagnetic action density,  $s(d_{AF}, N)/s(0, N)$ . The phase angle has been chosen to be  $\alpha = \pi/4$  for  $N = 4$  to minimize the action and  $s = \sin \pi/N$ ,  $N > 4$ . Since  $s(0, N) < 0$  the antiferromagnetic phase is preferred against the ferromagnetic one whenever the corresponding expression in the table is larger than 1.

## FIGURES

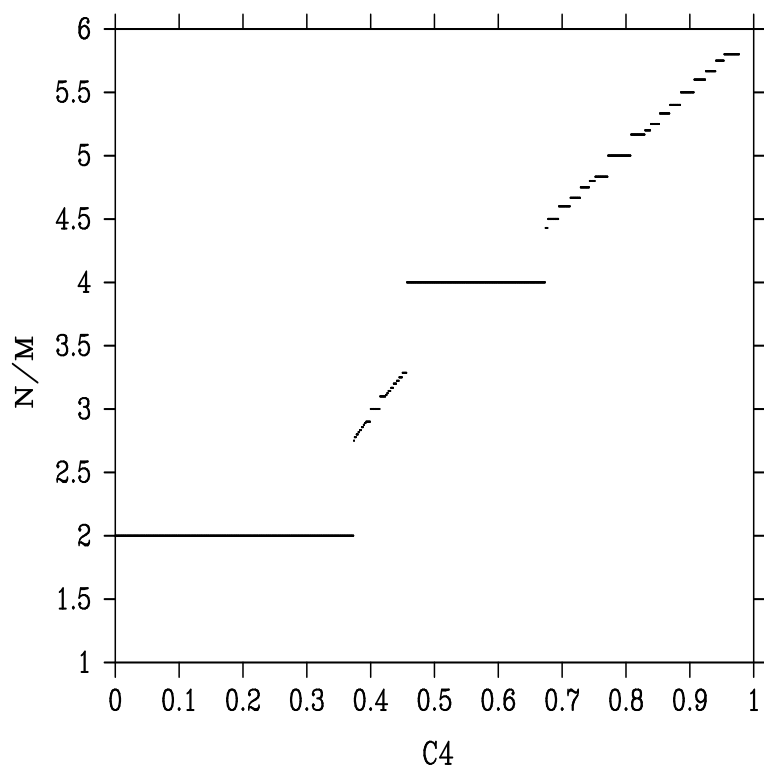


FIG. 1. The devil's staircase, the  $c_4$  dependence of the period length of the vacuum at  $c_2 = 2$ .

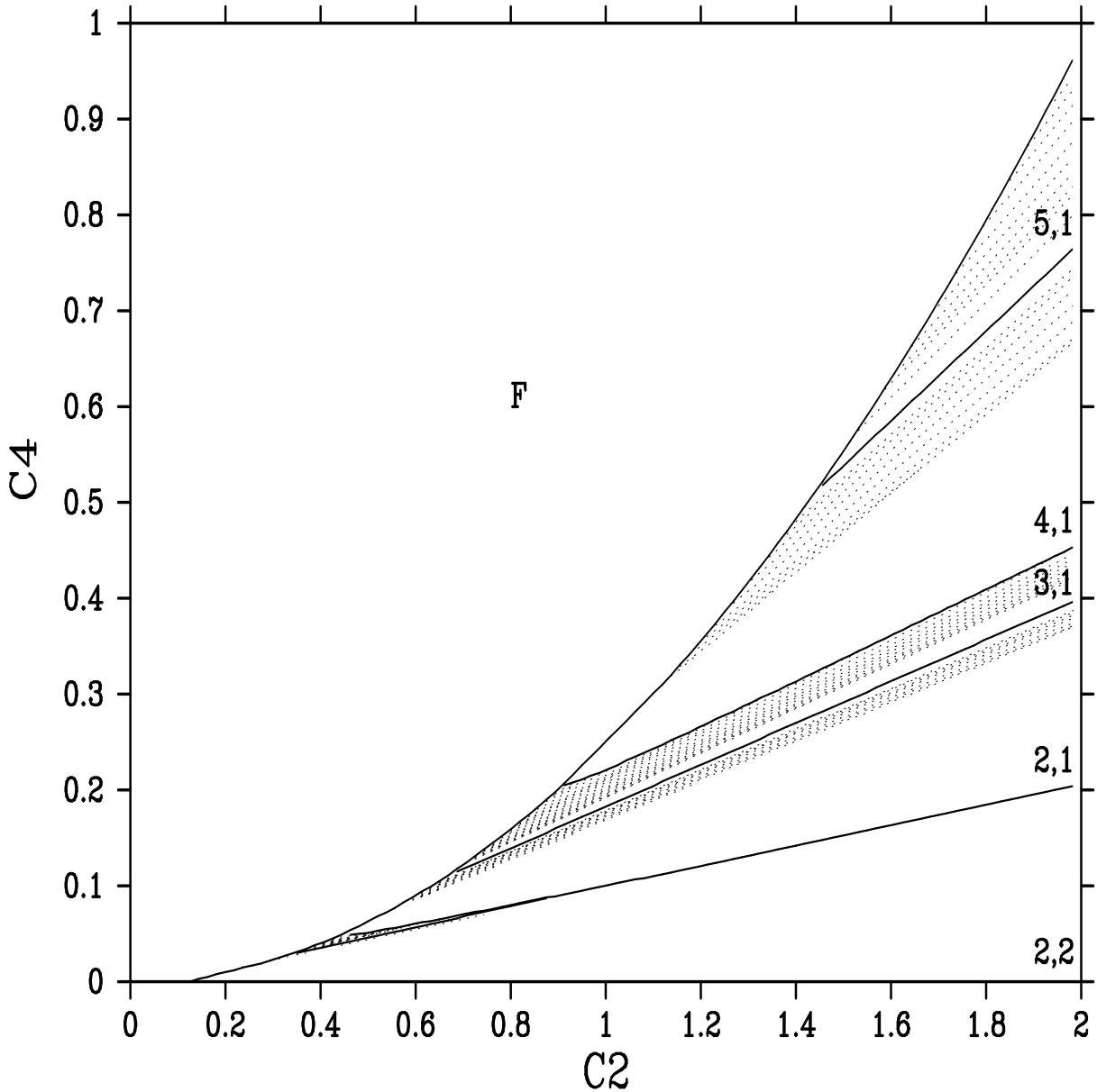


FIG. 2. The mean field phase structure in the  $(c_2, c_4)$  plane. F denotes the ferromagnetic phase. The lower edges of the phases with  $M = 1$  and  $M > 1$  are indicated by solid and dashed lines, respectively. The values of  $N, d_{AF}$  are shown for  $M = 1$  at the right.

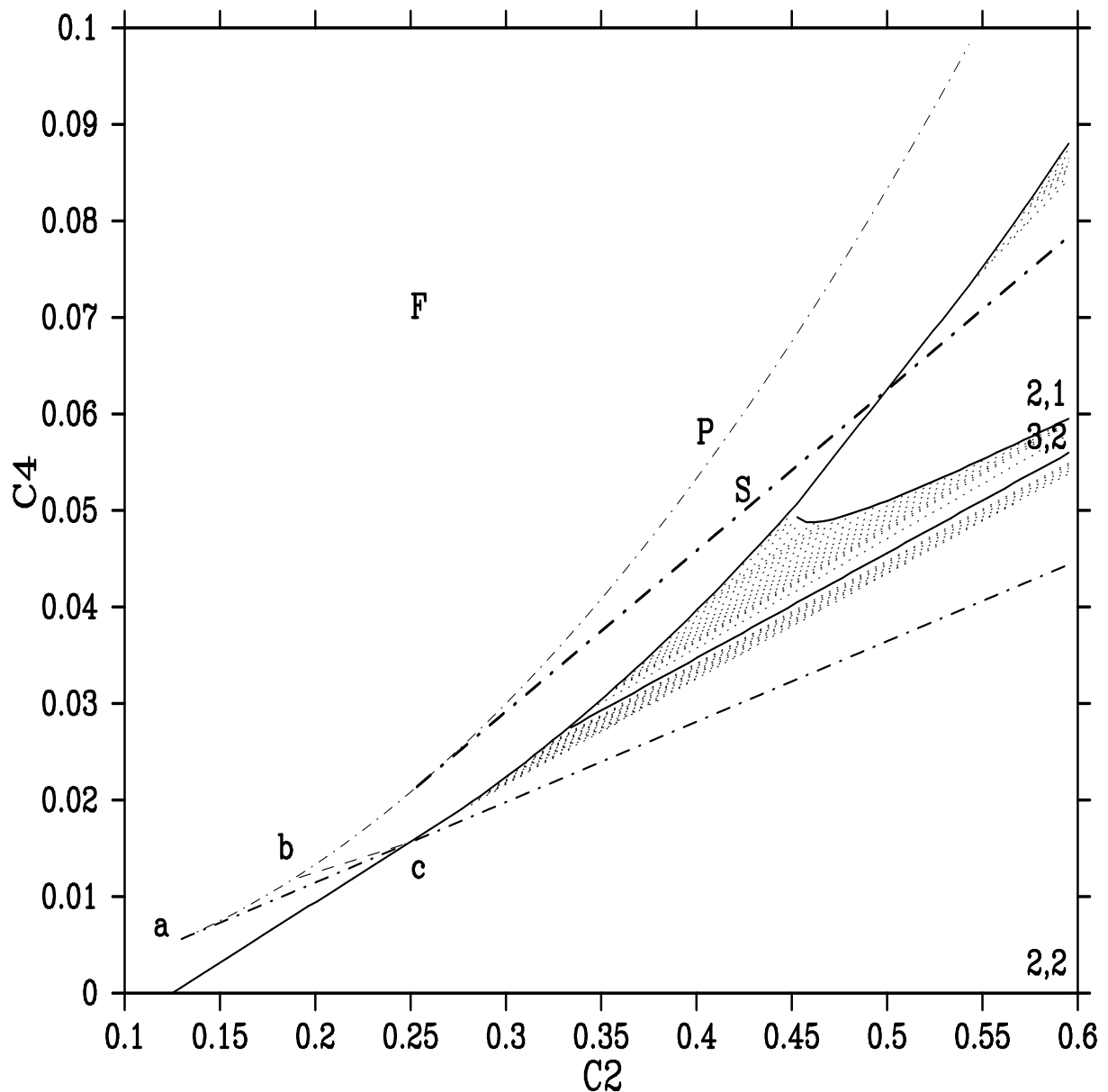


FIG. 3. The zoom into the mean field phase diagram with the regions characterizing the different behaviour of the propagator.

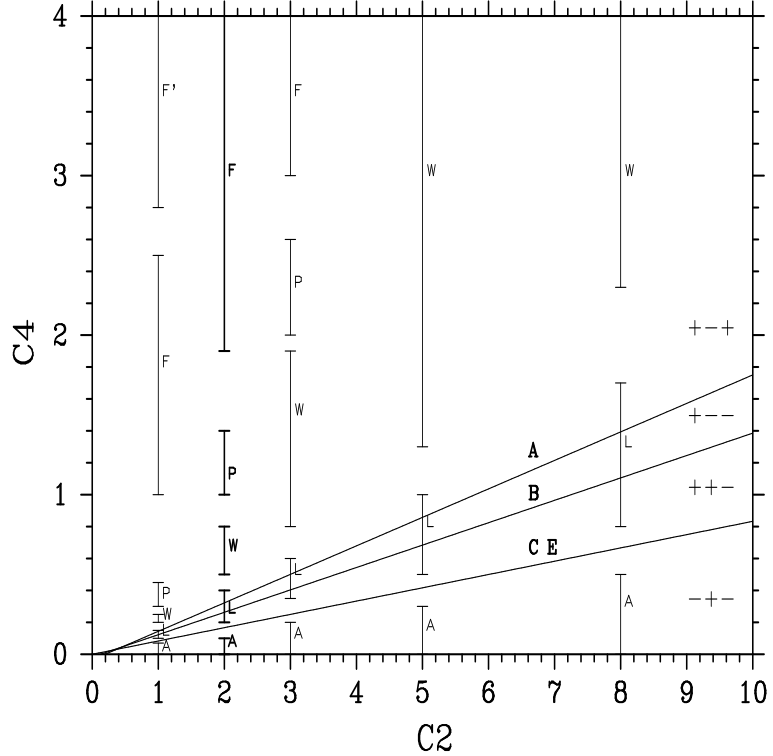
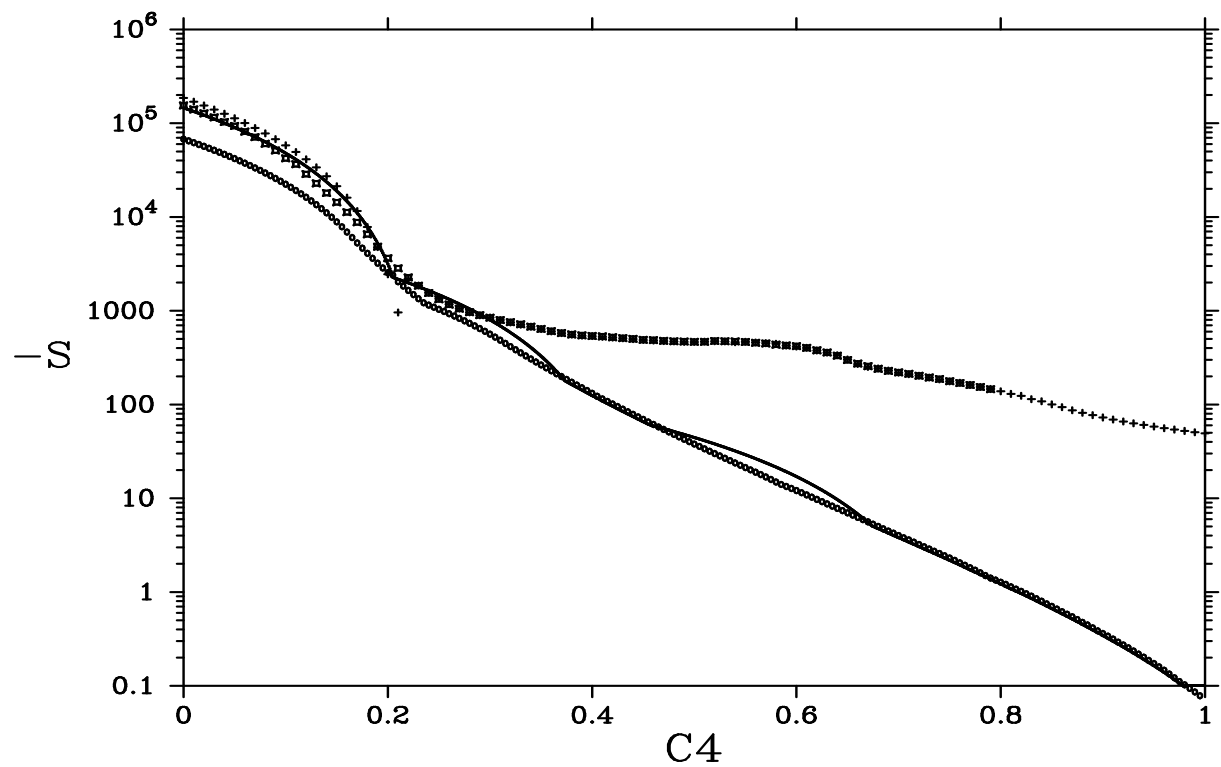
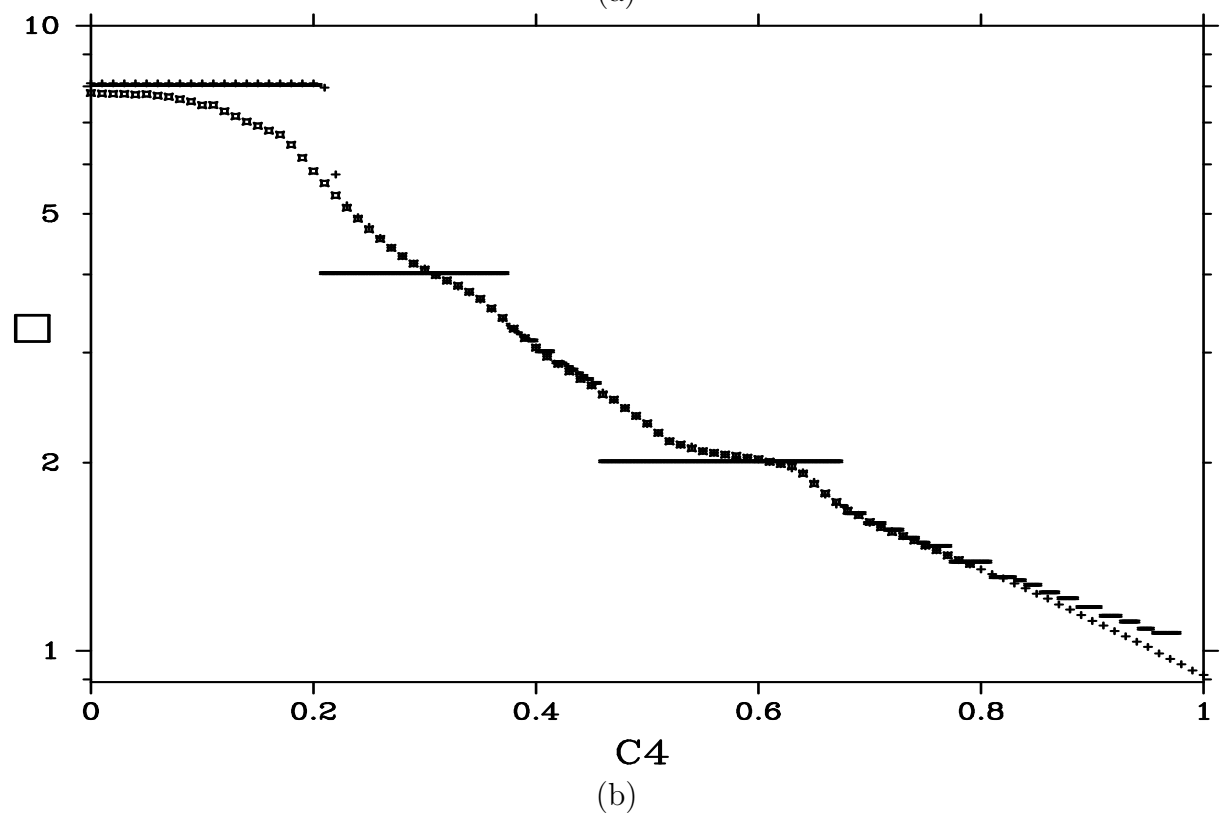


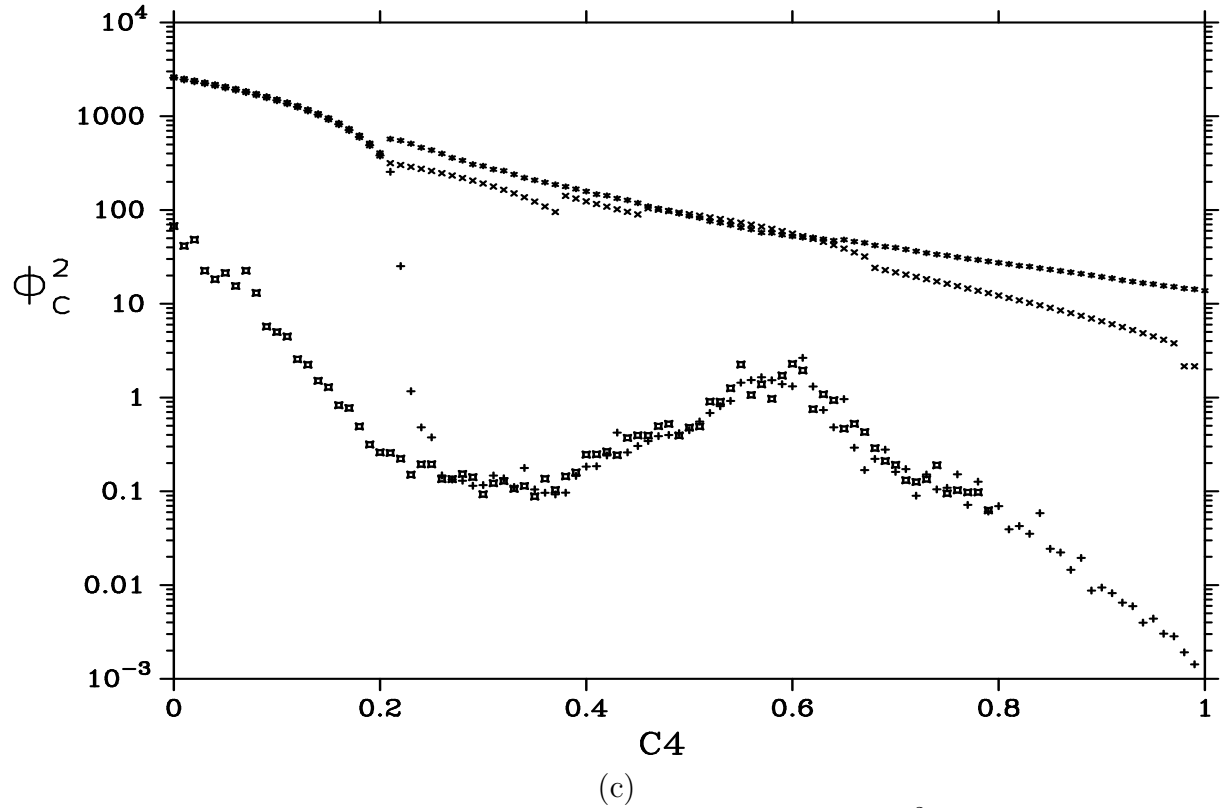
FIG. 4. The phase structure and the frustrations on the plane  $(c_2, c_4)$ . The lines where the coefficients  $A$ ,  $B$ ,  $C$  and  $E$  of the lattice action change sign in the  $(c_2, c_4)$  plane. The letters along the vertical lines are to indicate the qualitative space-time structure of the vacuum seen in the simulation:  $A$ =ordered  $N=2$  antiferromagnetic;  $L$ =labyrinths;  $W$ =plane waves;  $P$ =weakly antiferromagnetic (onset of the crossover on the finite lattice),  $F$ =ferromagnetic and  $F'$ =weakly ferromagnetic.



(a)

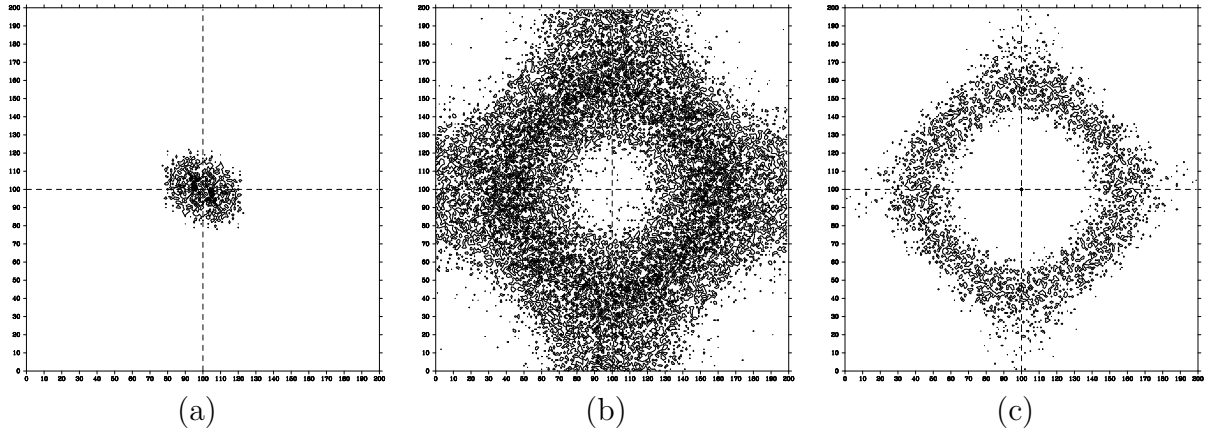


(b)



(c)

FIG. 5. Averages at  $c_2 = 2$ , (a): the action density,  $- \langle S \rangle / L^2$ , (b): the wavelength of the modulation of the vacuum, measured by  $- \langle \phi \square \phi \rangle / \langle \phi^2 \rangle$ , (c): the amplitude of the modulation.



(b)

(c)

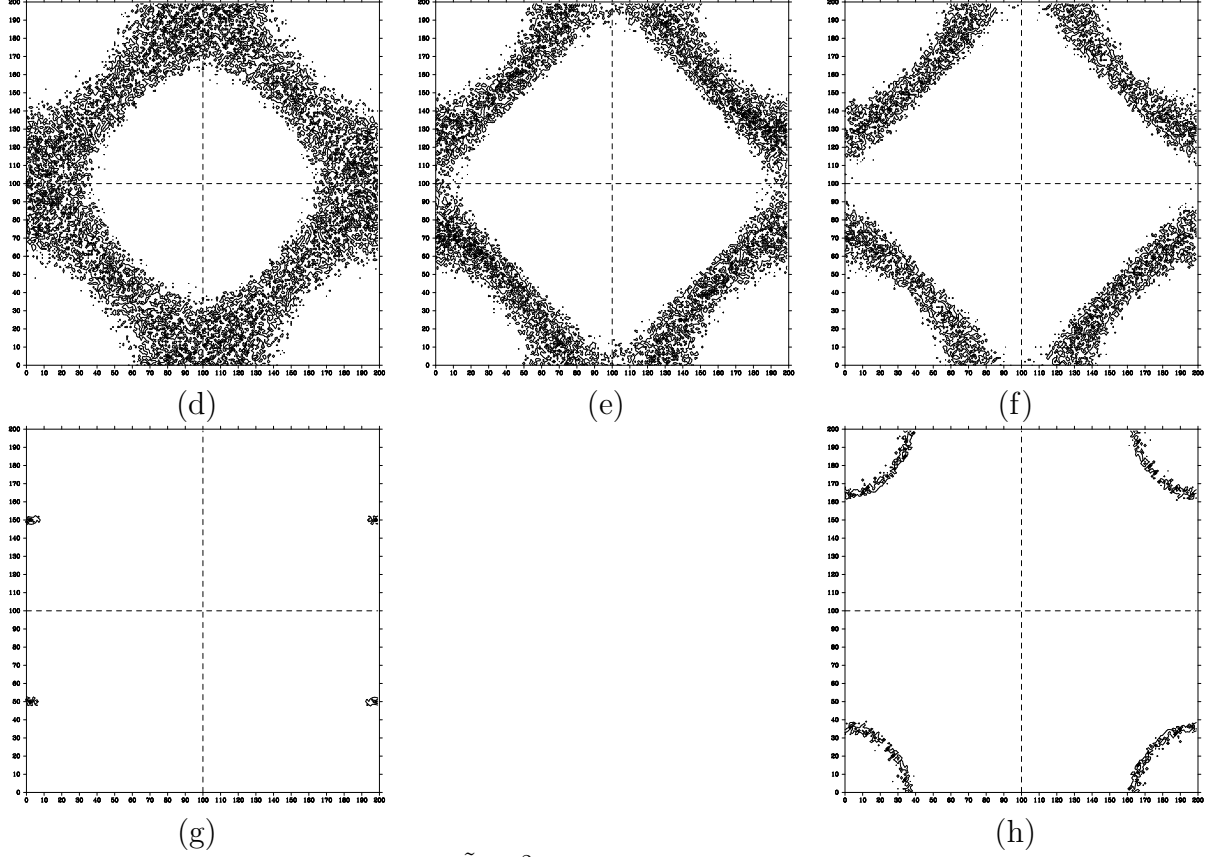


FIG. 6. The Fourier transform  $\langle |\tilde{\phi}(p)|^2 \rangle$  in the plane  $(p_1, p_2)$  for  $c_2 = 2$ . Disordered initial conditions: (a):  $c_4 = 0.06$ ; (b):  $c_4 = 0.23$ . Ordered initial conditions: (c):  $c_4 = 0.23$ ; (d):  $c_4 = 0.31$ ; (e):  $c_4 = 0.38$ ; (f):  $c_4 = 0.39$ ; (g)  $c_4 = 0.57$ ; (h):  $c_4 = 0.9$ .